

P-2620



Structural behaviour of reinforced Geopolymer concrete



A Project Report

Submitted by

Santo sebastian

-

0720101011

in partial fulfillment for the award of the degree
of



**Master of Engineering
in
Structural Engineering**

**DEPARTMENT OF CIVIL ENGINEERING
KUMARAGURU COLLEGE OF TECHNOLOGY
COIMBATORE – 641 006
(An Autonomous Institution Affiliated to Anna University, Coimbatore.)**

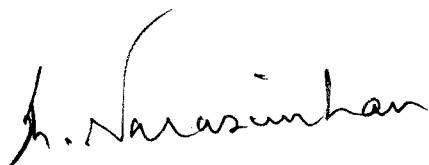
ANNA UNIVERSITY: COIMBATORE

MAY 2009

ANNA UNIVERSITY: COIMBATORE

BONAFIDE CERTIFICATE

Certified that this project report entitled “Structural behaviour of reinforced geopolymer concrete” is the bonafide work of Mr. Santo Sebastian-Register No. 0720101011 who carried out the project work under my supervision.



Dr.S.L.Narasimhan

Head of Department

Department of Civil engineering

Kumaraguru College of Technology

Coimbatore-641 006



Dr.D.L. venkatesh Babu,

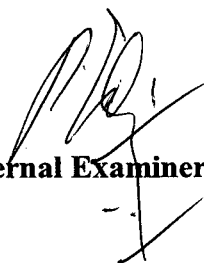
Professor, Thesis supervisor

Department of Civil engineering

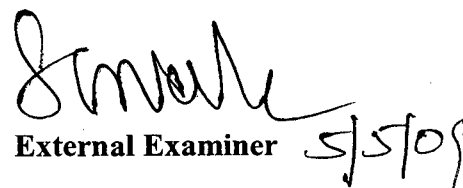
Kumaraguru College of Technology

Coimbatore-641 006

Certified that the candidate with university Register No. 0720101011 was examined in project viva voce Examination held on 05-05-2009



Internal Examiner



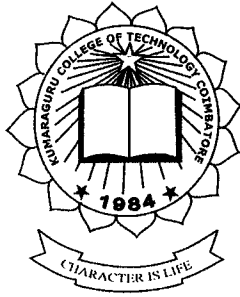
External Examiner

DEPARTMENT OF CIVIL ENGINEERING
KUMARAGURU COLLEGE OF TECHNOLOGY, COIMBATORE 641 006

(An Autonomous Institution Affiliated to Anna University, Coimbatore.)

CERTIFICATE





KUMARAGURU COLLEGE OF TECHNOLOGY COIMBATORE , TAMILNADU



DEPARTMENT OF CIVIL ENGINEERING
INNOVATIONS IN CIVIL ENGINEERING - ICE'09

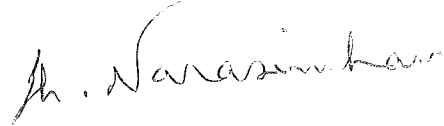
CERTIFICATE

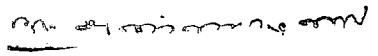
This is to certify that Mr/Ms Santo Sebastian - PA student
of Kumaraguru College of Technology, Coimbatore
has participated and presented a paper in the National Conference on
"INNOVATIONS IN CIVIL ENGINEERING - ICE'09" during 21st, April 2009.

Title Study on the properties of Fly Ash Based
Geopolymer Concrete.



Dr.P.ESWARAMOORTHY & Mrs.K.RAMADEVI
COORDINATORS


Dr.S.L.NARASIMHAN
CONVENOR


Prof.R.ANNAMALAI
VICE PRINCIPAL



ACC Limited
Sales Unit
50, Kamaraj Road, Redfields,
P.B.No. 3924, Opp.Nirmala College,
Coimbatore - 641 018. India

Phone +91 422 2223156
Fax +91 422 2222911
www.acclimited.com

Date: 29-04-09

To whomsoever it may concern

This is to certify that **Mr. Santo Sebastian** (Roll No. 0720101011), final year student of Master of Structural engineering from Kumaraguru College of Technology, Coimbatore has successfully completed a project titled “**Structural Behaviour of Reinforced Geopolymer concrete**” during the period of December 2008 to March 2009.

The processed fly ash of required quantity and technical support for this project has been sponsored by m/s ACC Limited, SU- Coimbatore.

We wish him success in all his future endeavors.

For ACC Ltd,

A Sudhahar,
Assistant Manager,
SU Coimbatore

ABSTRACT

ABSTRACT

Concrete, an essential building material is widely used in the construction of infrastructures such as buildings, bridges, highways, dams, and many other facilities. One of the ingredients usually used as a binder in the manufacture of concrete is the Ordinary Portland Cement (OPC). However, the manufacturing of the Portland cement is an energy intensive process and releases a very large amount of green house gas to atmosphere. To reduce greenhouse gas emissions, efforts are needed to develop environmentally friendly construction materials. Geopolymer concrete is produced without the presence of Portland cement as a binder. Instead, the base material such as fly ash, that is rich in Silicon (Si) and Aluminum (Al), is activated by alkaline solution to produce the binder. It binds the loose coarse and fine aggregates, and other unreacted materials in the mixture.

The experimental work involved flexural testing of beams and axial load testing of columns of both geopolymer and Portland cement concrete. The compressive strength of geopolymer and Portland cement concrete was about 20MPa. The test results included the flexural strength, crack pattern and deflection of beam. It also included load carrying capacity, axial stress-strain characteristics of columns. The test results presented in this report shows that steam-cured low-calcium fly ash-based geopolymer concrete has excellent compressive strength and is suitable for structural applications. The elastic properties of GPC and the behaviour and strength of reinforced structural members are similar to those of Portland cement concrete (OPC). The design provisions contained in the current standards and codes are used to design reinforced fly ash-based geopolymer concrete structural members. The applications of geopolymer concrete and future research needs are also identified. It can be used in many infrastructure applications. One ton of low-calcium fly ash can be utilized to produce about 2.5 cubic meters of high quality geopolymer concrete and the bulk price of chemicals needed to manufacture this concrete is cheaper than the bulk price of one ton of Portland cement. Given the fact that fly ash is considered as a waste material, the low-calcium fly ash-based geopolymer concrete is, therefore, cheaper than the Portland cement concrete.

ACKNOWLEDGEMENT

ACKNOWLEDGEMENT

First and foremost I submit my thanks to **The Almighty**, through whom all things are possible. This work was not by my might nor by power, but by **His spirit**. This work not be possible without the gifts, **God** has given to me.

I take pride and immense pleasure in expressing my deep sense of gratitude and indebtedness to my guide **Dr.D.L.Venkatesh Babu**, Professor, department of Civil engineering, for contributing to my project work in numerous ways through his constant source of motivation, wise counsel and encouragement which has been an inspiration throughout the work for the successful completion of this research work.

I express my sincere gratitude to **Er. A. Sudhahar**, Assistant manager, ACC Ltd, for his support, valuable suggestions, and providing processed fly ash of required quantity for carrying out this thesis work.

I deem great pride in expressing heartfelt gratitude to **Dr. S.L. Narasimhan**, H.O.D, Department of Civil engineering, for allowing me to do this project and the facilities extended throughout the work.

I express my profound gratefulness to **Prof.R.Annamaiai**, vice principal for providing the necessary facilities for the successful completion of this thesis work.

I thank to **Dr.S.Sadasivam**, Dean academic, for funding the project as KCT-R&D-management funded project.

Words are inadequate in offering my thanks to **Dr. P. Eswaramoorthy**, project Coordinator, and **Ms. R. Manju**, class advisor.

I am sincerely thanks to **Mr. G. Ganeshmoorthy**, supporting staff of Structural technology Center, for helping in carry out the experimental work.

I would be failing in my duty if I do not express my gratitude of **all those authors** who had contributed abundant literature through various research papers, books, etc. in many international, national journals and conferences.

Last but not least, I thank one and all those who have rendered help directly or indirectly at various stages of thesis.

CONTENTS



CONTENTS

Title	Page No
Bonafide Certificate	ii
Certificate	iii
Abstract	iv
Acknowledgement	v
Contents	vi
List of Tables	ix
List of Figures	x
List of Abbreviations	xiii
CHAPTER 1 INTRODUCTION	
1.1 General	1
1.2 Background of the project	2
1.3 Geo-polymers	3
1.3.1 Geo-polymerisation	3
1.3.2 Chemistry of geopolymer	4
1.4 Research objectives	8
1.5 Scope of work	8
1.6 Report arrangement	9
CHAPTER 2 LITERATURE REVIEW	10
CHAPTER 3 MATERIAL PROPERTIES	13
3.1 Material used	13
3.1.1 Fly ash	13
3.1.2 Alkaline solution	15
3.1.3 Aggregates	16
3.1.3.1 Test on fine aggregate	16

Title	Page No
3.1.3.2 Test on coarse aggregate	17
3.2 Mixture proportion geopolymer concrete	19
3.3 Reinforcing bars	24
CHAPTER 4 MAIN THEME OF PROJECT	25
4.1 Introduction	25
4.2 Experimental programme	25
4.2.1 Beams	25
4.2.1.1 Geometry and reinforcement configuration	25
4.2.1.2 Specimen manufacture and curing process	25
4.2.1.3 Test set up and instrumentation	29
4.2.1.3 Test procedure	29
4.2.2 Columns	30
4.2.2.1 Geometry and reinforcement configuration	30
4.2.2.2 Specimen manufacture and curing process	31
4.2.2.3 Test set up and instrumentation	34
4.2.2.4 Test procedure	34
CHAPTER 5 PRESENTATION AND DISCUSSION OF RESULTS	36
5.1 Test result on fresh concrete	36
5.2 Test result on hardened concrete	36
5.2.1 Compressive strength	36
5.2.2 Split tensile strength	38
5.3 Beams	39
5.3.1 General observations	39

Title	Page No
5.3.2 Flexural capacity	40
5.3.3 Cracking moment	42
5.3.4 Deflection	43
5.3.5 Ductility	48
5.4 Columns	49
5.4.1 General observations	49
5.4.2 Load carrying capacity	50
5.4.3 Axial Stress-Strain Curve For PPC-C1 and GPC-C1	51
5.4.4 Axial Stress-Strain Curve For PPC-C2 and GPC-C2	53
5.4.5 Crack pattern and failure mode	53
CHAPTER 6 CONCLUSIONS	55
6.1 General conclusions	55
6.2 Specific conclusions	55
6.2.1 Reinforced geopolymer concrete beams	55
6.2.2 Reinforced geopolymer concrete columns	56
REFERENCES	
APPENDIX A	
APPENDIX B	
APPENDIX C	
APPENDIX D	

LIST OF TABLES

LIST OF TABLES

Table	Title	Page No.
3.1	Chemical Composition of Fly Ash	14
3.2	Composition of alkaline solution	16
3.3	Properties of fine aggregates	17
3.4	Properties of coarse aggregate	17
3.5	Mixture proportion of Geopolymer concrete (GPC)	20
3.6	Mix proportion of Portland Pozzolona cement concrete (PPC)	20
3.7	Properties of steel reinforcement	24
3.8	Characteristics of steel reinforcement	24
4.1	Beam specimen details	26
4.2	Column specimen details	30
5.1	Results of compaction factor values for GPC	36
5.2	Test result of compressive strength test of GPC	37
5.3	Comparison between steam curing and oven curing	38
5.4	Test result of split tensile strength test of GPC	39
5.5	Comparison between experimental and theoretical Ultimate moment of GPC beams	41
5.6	Percentage reduction in Ultimate load carrying capacity of GPC beams	41
5.7	Cracking characteristics of beams	43
5.8	Displacement Ductility of beams obtained from experiment	49
5.9	Ultimate load of column beam specimen	51

LIST OF FIGURES

LIST OF FIGURES

Figure	Title	Page No.
1.1	Computer molecular graphics of polymeric Mn-(-Si-O-Al-O-) _n poly (sialate)	5
1.2	Chemical structures of polysialates	7
3.1	Class F Fly Ash	18
3.2	Fine Aggregates	18
3.3	Coarse Aggregates	18
3.4	Sodium Hydroxide pellets	18
3.5	Sodium silicate Solution	18
3.6	Alkaline solution	18
3.7	Dry mixing of GPC	21
3.8	Wet mixing GPC	21
3.9	Steam Curing chamber	21
3.10	Hot air oven	21
3.11	Mould with GPC	22
3.12	Oven curing of specimens	22
3.13	Cylinders after curing	22
3.14	Cubes after curing (GPC-1)	22
3.15	Cubes after curing (GPC-2)	23
3.16	Compressive strength test	23
3.17	Split tensile strength test	23
4.1	Geometry and reinforcement details	26

Figure	Title	Page No.
4.2	Reinforcement cages	27
4.3	Mould with reinforcement	27
4.4	GPC after mixing	27
4.5	Compaction using needle vibrator	27
4.6	GPC in beam mould	28
4.7	Steam curing with mould	28
4.8	Steam curing without mould	28
4.9	Beam specimens after finishing	28
4.10	Bending test of beams	29
4.11	Geometry and reinforcement details of column	30
4.12	Reinforcement cages	32
4.13	Mould with reinforcement	32
4.14	GPC after mixing	32
4.15	Compaction using needle vibrator	32
4.16	GPC in column mould	33
4.17	Steam curing with column mould	33
4.18	Steam curing without mould	33
4.19	Column specimens after finishing	33
4.20	Test configuration of column	34
5.1	Graphical comparison of ultimate moment of GPC and PPC	42
5.2	Idealised load-deflection curve of beam	44
5.3	Crack pattern and failure mode of beam PPC-B1	45
5.4	Crack pattern and failure mode of beam PPC-B2	45
5.5	Crack pattern and failure mode of beam GPC-B1	46
5.6	Crack pattern and failure mode of beam GPC-B2	46

Figure	Title	Page No.
5.7	Load versus Mid-span deflection of beams PPC-B1 and GPC-B1	47
5.8	Load versus Mid-span deflection of beams PPC-B2 and GPC-B2	47
5.9	Load versus Mid-span deflection of beams PPC-B3 and GPC-B3	48
5.10	Failure Mode of Short Column	50
5.11	Typical stress-strain curves for uniaxially loaded short column	52
5.12	Axial stress-strain curves for PPC-C1 and GPC-C1 Column specimen	52
5.13	Axial stress-strain curves for PPC-C2 and GPC-C2 Column specimen	53
5.14	Failure mode of GPC-C1	54
5.15	Failure mode of PPC-C1	54

*LIST OF SYMBOLS AND
ABBREVIATIONS*

LIST OF SYMBOLS AND ABBREVIATIONS

ACI	- American Concrete Institute
ASTM	- American standard for testing Materials
C.F	- Compaction Factor
CSH	- Calcium Silicate Hydrate
f_{cr}	- Modulus of rupture
GPC	- Geopolymer Concrete
HVFA	- High Volume Fly Ash
HYSD	- High Yield Strength Deformed
IS	- Indian Standards
I_T	- Second moment of area of the transformed concrete section with reinforcement with reference to NA
LVDT	- Linear Variable Differential Transducer
M	- Molar
$M_{cr (exp)}$	- Experimental Cracking moment
$M_{cr (theo)}$	- Theoretical cracking moment
M_{ult}	- Experimental Ultimate moment
M_{ides}	-Theoretical Design moment
Y_t	- Distance between the neutral axis and the extreme tension fiber
Δ_y	- Deflection at Yield stage
Δ_u	- Deflection at Ultimate stage

INTRODUCTION



CHAPTER 1

INTRODUCTION

1.1 GENERAL

Concrete is the most commonly used construction material. Demand for concrete as construction material is on the increase so as the production of cement. The production of cement is increasing about 3% annually. Customarily, concrete is produced by using Portland cement as the binder. However, the manufacturing of the Portland cement is an energy intensive process and releases a very large amount of green house gas to atmosphere. Production of one ton of Portland cement requires about 2.8 ton raw materials, including fuel and other materials and generates 5 to 10 % of dusts. Altogether 6000–14000 m³ dust-containing air-streams are generated per ton cement manufacture, which contain between 0.7 to 800 g/m³ of dust and accounts for about one ton of green house gas CO₂ released to the atmosphere as a result of de-carbonation of lime in the kiln during manufacturing of cement (Eq. 1).



Also the greatest problem faced by industries, as far as waste disposal is concerned is the safe and effective disposal of its effluent, sludge and by-products such as large quantities of fly ash that are produced during the combustion of coal used for electricity generation. It is estimated that by the year 2010, the amount of the fly ash produced will be about 780 million tones annually. Most of this ash is disposed in landfills at suitable sites. Land filling is not a desirable option because it not only causes huge financial burden to the foundries, but also makes them liable for future environmental costs and problems associated with land filling regulations. The increasing load of toxic metals in the landfill potentially increases the threat to ground water contamination. Increasing economic factors also dictate that industry should look forward to recycling and reuse of waste material as a better option to land filling and discarding.

Need exists for a technology that can easily and cheaply handle large quantities of waste materials and by-products containing heavy metals as an alternative to OPC (ordinary Portland cement). Disposal of hazardous waste must meet at least two conditions (1) Safe chemical encapsulation i.e. control their release into ground water and seepage water. (2) Structural stability with respect to adverse environmental condition. To overcome these problems, geopolymer emerged as a possible solution for using the by-products and could be utilized to manufacture precasts structure and non-structural elements, concrete pavements, concrete products and immobilization of toxic waste that are resistant to heat and aggressive environment. Therefore, there are efforts to develop the other form of cementitious materials for producing concrete. Geopolymer concrete is produced without the presence of Portland cement as a binder. Instead, the base material such as fly ash, that is rich in Silicon (Si) and Aluminum (Al), is activated by alkaline solution to produce the binder. The replacement of clinker by pozzolanic materials and the use of new alternative binders are two of the various methods from which the Portland cement industry may benefit in its attempt to lower CO₂ emissions.

1.2 BACKGROUND OF PROJECT

Portland cement concrete is a mixture of Portland cement, aggregates, and water. Concrete is the most often-used construction material. The worldwide consumption of concrete was estimated to be about 8.8 billion tons per year (Metha2001). Due to increase in infrastructure developments, the demand for concrete would increase in the future. The manufacture of Portland cement releases carbon dioxide (CO₂) that is a significant contributor of the greenhouse gas emissions to the atmosphere. The production of every tone of Portland cement contributes about one tone of CO₂. Globally, the world's Portland cement production contributes about 1.6 billion tons Of CO₂ or about 7% of the global loading of carbon dioxide into the atmosphere (Metha 2001, Malhotra 1999; 2002). By the year 2010, the world cement consumption rate is expected to reach about 2 billion tonnes, meaning that about 2 billion tons CO₂ will be released. In order to address the environmental effect associated with Portland cement, there is a need to use other binders to make concrete.

One of the efforts to produce more environmentally friendly concrete is to replace the amount of Portland cement in concrete with by-product materials such as fly ash. An important achievement in this regard is the development of high volume fly ash (HVFA) concrete that utilizes up to 60 percent of fly ash, and yet possesses excellent mechanical properties with enhanced durability performance. The test results show that HVFA concrete is more durable than Portland cement concrete (Malhotra 2002). Another effort to make environmentally friendly concrete is the development of inorganic alumina-silicate polymer, called Geopolymer, synthesized from materials of geological origin or by-product materials such as fly ash that are rich in silicon and aluminum (Davidovits 1994, 1999). Fly ash, one of the source materials for geopolymer binders, is available abundantly worldwide, but to date its utilization is limited. From 1998 estimation, the global coal ash production was more than 390 million tons annually, but its utilization was less than 15% (Malhotra 1999). In the USA, the annual production of fly ash is approximately 63 million tons, and only 18 to 20% of that total is used by the concrete industries (ACI 232.2R-03 2003). In the future, fly ash production will increase, especially in countries such as China and India. Just from these two countries, it is estimated that by the year 2010 the Production of the fly ash will be about 780 million tones annually (Malhotra 2002). Accordingly, efforts to utilize this by-product material in concrete manufacture are important to make concrete more environmentally friendly. For instance, every million tons of fly ash that replaces Portland cement helps to conserve one million tons of lime stone, 0.25 million tonnes of coal and over 80 million units of power, not withstanding the abatement of 1.5 million tonnes of CO₂ to atmosphere (Bhanumathidas and Kalidas 2004).

1.3 GEOPOLYMERS

1.3.1 Geopolymerisation

Geopolymerization is a geosynthesis (reaction that chemically integrates minerals) that involves naturally occurring silico-aluminates. Any pozzolanic compound or source of silica and alumina, which is readily dissolved in the alkaline solution, acts as a source of geopolymer precursor species and thus lends itself to geopolymerization. The alkali component as an activator is a compound from the element of first group in the

periodic table, so such material is also called as alkali activated aluminosilicate binders or alkali activated cementitious material. Silicon and aluminum atoms react to form molecules that are chemically and structurally comparable to those building natural rocks. The inorganic polymeric material can be considered as an amorphous equivalent of geological feldspars, but synthesized in a manner similar to thermosetting organic polymers. For this reason, these materials are termed as “geopolymers”. It offers attractive option for simple industrial applications where large volume of waste materials needs to be stabilized. It is named because of the similarities with the organic condensation polymers as far as their hydrothermal synthesis conditions are concerned. Study of the literature and patents demonstrated that before 1978, the idea of using this mineral chemistry for the development of a mineral polymer had been totally neglected. As a function of chemical composition of initial materials, the alkaline cements are classified into two groups. (i) Binders synthesized from materials rich in calcium such as blast furnace slag that produces calcium silicate hydrate (CSH) gel when activated with alkaline solution. (ii) Materials synthesized with raw materials low in calcium and rich in SiO₂ and Al₂O₃ such as metakaolin. These materials when activated with alkaline solution, formation of an amorphous material (alkaline aluminosilicate) that develops high mechanical strength at early ages after a soft thermal curing. These materials differ substantially from ordinary Portland cement, as they use totally different reaction pathway in order to attain structural integrity. Pozzolanic cement depends on the presence of calcium-silicate hydrate for matrix formation and strength where as geopolymers utilize the polycondensation of silica and alumina precursors (fly ash, kaolin, metakaolin) and a high alkali content to attain structural strength.

1.3.2 Chemistry of Geopolymer

Geopolymerization is based on chemistry of alkali activated inorganic binders, which were accidentally discovered by Purdon. He studied the sodium hydroxide on a variety of minerals and glasses containing silicon and/or aluminum and summarized it in two steps ;(1) liberation of silica, alumina and lime and (2) formation of hydrated calcium silicates, aluminates as well as regeneration of caustic solution. The hardening mechanism of alkali activated aluminosilicate binder involves dissolution of Si or Al in

the presence of sodium hydroxide, and precipitation of calcium silicate or aluminum hydrate with the generation of sodium hydroxide. Similarly, Glukhovskiy identified both CSH and calcium and alumino-silicate hydrate as solidification product on the alkali activation of slag binders and concluded that clay mineral reacts during alkali treatment to form aluminosilicate hydrate. Finally, Davitovits developed a kind of mineral polymer material with 3-D cross-linked polysialate chain, which resulted from the hydroxylation and polycondensation reaction of natural minerals such as clay, slag, fly ash and pozzolan on alkaline activation below 160 °C (Figure 1).

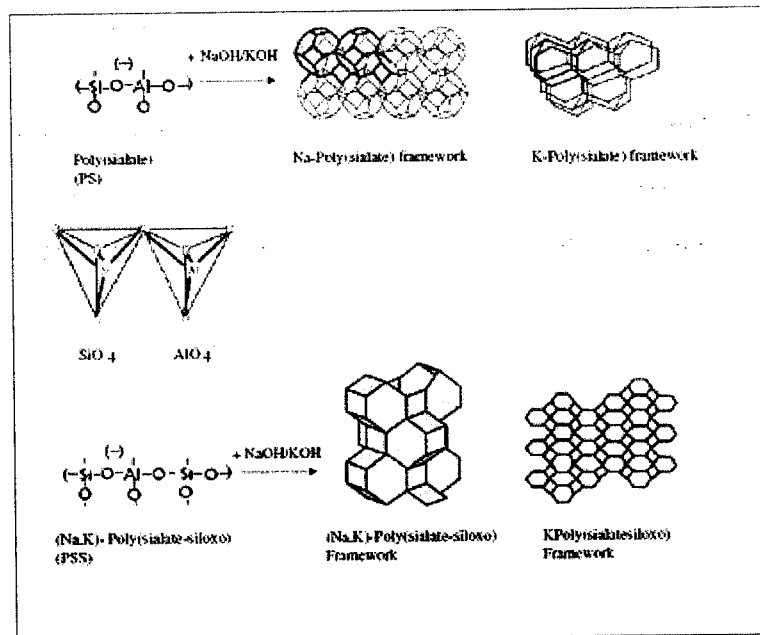


Figure 1.1 Computer molecular graphics of polymeric Mn-(-Si-O-Al-O-) _n poly (sialate)

This inorganic polymer was first named polysialate in 1976 and later coined as “Geopolymer”. In 1980 the setting reaction of alkali activated slag cement was explained. Recently, Deventer has contributed towards the development and applications of geopolymers. Mechanism of geopolymers involves the polycondensation reaction of geopolymeric precursors i.e. alumino-silicate oxide with alkali polysilicates yielding polymeric Si-O-Al bond (Eq. 2)



Where M is the alkaline element and n is the degree of polycondensation. Davitovits has suggested that certain synthesis limits existed for the formation of strong products; satisfactory compositions lay in the range M_2O/SiO_2 , 0.2 to 0.48; SiO_2/Al_2O_3 , 3.3 to 4.5; H_2O/M_2O , 10–25; and M_2O/Al_2O_3 , 0.8 to 1.6. The geopolymeric alumino-silicate has been grouped in three families depending on the atomic ratio Si/Al that may be 1, 2, or 3. Geopolymers consist of aluminum and silica tetrahedrally interlinked alternately by sharing all the oxygen atoms. A polymeric structure of Al–O–Si formed constitutes the main building blocks of geopolymeric structure.

Alkali metal salts and/or hydroxide are necessary for the dissolution of silica and alumina as well as for the catalysis of the condensation reaction. The gel phase is thought to be highly reactive and produced by co-polymerization of individual alumina and silica from their source, dissolved by the alkali metal. Some cations must be present to keep the structure neutrality (since aluminum is four fold). Na, K, Ca and other metallic cations maintain this neutrality. It is still not clear whether these ions simply play a charge-balancing role or are actively bonded into the matrix. The mechanism of immobilization is expected to be the combination of chemical and physical interaction. Cation is either bonded into the matrix via Al–O or Si–O bond or present in the framework cavities to maintain electrical charge balance. A physically encapsulated cation should be substituted by another cation if its surrounding allows the diffusion process to occur. Amorphous to semi-crystalline three dimensional alumino-silicate structures are of the poly(sialate) type (Si–O–Al–O–), the poly(sialate-siloxo) type (Si–O–Al–O–Si–O–), the poly(sialate-disiloxo) type (Si–O–Al–O–Si–O–Si–O–) as shown in Figure 2.

Although in some cases strength develops slowly. Geopolymers are very similar to zeolites and are formed in similar manner as zeolites do. There exists a difference between zeolite formation and geopolymerization as related to the composition of the initial reaction mixtures. Zeolites usually form in closed hydrothermal systems but geopolymers do not. Geopolymers are amorphous to semi-crystalline, where as zeolites are usually crystalline in nature. When fly ash in geopolymers is mixed with the alkaline dissolution; a vitreous component is quickly dissolved. In such a situation there is not sufficient time and space for the gel to grow into a well-crystallized structure resulting in a microcrystalline, amorphous or semi-amorphous structure. Aluminum source react with calcium hydroxide via a pozzolanic reaction to produce CSH and calcium alumino silicate which are chemically less reactive. Zeolites usually crystallize from dilute aqueous solution, where precursor species have mobility as well as enough time to undergo proper orientation and alignment before bonding into a crystal structure.

1.4 RESEARCH OBJECTIVES

The primary objectives of this research are to conduct experimental and analytical studies to establish the following

- a) The flexural behaviour of reinforced geopolymer concrete beams including flexural strength, crack pattern, deflection and ductility.
- b) The behaviour and strength of reinforced geopolymer concrete short columns subjected to axial load.
- c) The comparison of above results with the *reinforced conventional* concrete beams and columns

1.5 SCOPE OF WORK

The scope of work involve the following

- a) Based on the trial and error procedure, select appropriate geopolymer concrete mixtures needed to fabricate the reinforced test beams and columns.

- b) Casting and testing of three simply supported reinforced geopolymer concrete and ordinary concrete beams under monotonically increasing load with the longitudinal steel reinforcement ratio as test variable.
- c) Casting and testing of two reinforced geopolymer concrete and ordinary concrete column under axial load with the lateral tie spacing as test variable.

1.6 REPORT ARRANGEMENT

The report contains six Chapters. Chapter 1 presents a brief introduction about geopolymers. Chapter 2 gives a review of literature on geopolymers. The materials used, their properties and mix proportion of geopolymer concrete are given in Chapter 3. The main theme of project describes in Chapter 4, it includes the specimen manufacture and test programme. Chapter 5 presents and discusses the test results. The conclusions of thesis are given in Chapter 6. The report ends with a list of References and Appendices containing the details of experimental data and graphs.

LITERATURE REVIEW



CHAPTER 2

LITERATURE REVIEW

Davidovits (1988) introduced the term 'geopolymer' in 1978 to represent the mineral polymers resulting from geochemistry. Geopolymer, an inorganic alumina-silicate Polymer is synthesized from predominantly silicon (Si) and aluminum (Al) material of geological origin or by-product material. The chemical composition of geopolymer materials is similar to zeolite, but they reveal an amorphous Microstructure (Davidovits 1999). During the synthesized process, silicon and aluminum atoms are combined to form the building blocks that are chemically and structurally comparable to those binding the natural rocks.

Davidovits and Sawyer (1985) used ground blast furnace slag to produce geopolymer binders. This type of binders patented in the USA under the title Early High-Strength Mineral Polymer was used as a supplementary cementing material in the production of precast concrete products. In addition, a ready-made mortar package that required only the addition of mixing water to produce a durable and very rapid strength gaining material was produced and utilized in restoration of concrete airport runways, aprons and taxiways, highway and bridge decks, and for several new constructions when high early strength was needed.

Geopolymer has also been used to replace organic polymer as an adhesive in strengthening structural members. Geopolymers were found to be fire resistant and durable under UV light (**Balaguru et al 1997**) **12 van Jaarsveld, van Deventer, and Schwartzman (1999)** carried out experiments on geopolymers using two types of fly ash. They found that the compressive strength after 14 days was in the range of 5 – 51 MPa. The factors affecting the compressive strength were the mixing process and the chemical composition of the fly ash. A higher CaO content decreased the microstructure porosity and, in turn, increased the compressive strength. Besides, the water-to-fly ash ratio also influenced the strength. It was found that as the water-to-fly ash ratio decreased the compressive strength of the binder increased.



Palomo, Grutzeck, and Blanco (1999) studied the influence of curing temperature, curing time and alkaline solution-to-fly ash ratio on the compressive strength. It was reported that both the curing temperature and the curing time influenced the compressive strength. The utilization of sodium hydroxide (NaOH) combined with sodium silicate (Na_2Si_3) solution produced the highest strength. Compressive strength up to 60 MPa was obtained when cured at 85°C for 5 hours.

Xu and van Deventer (2000) investigated the geopolymerization of 15 natural Al-Si minerals. It was found that the minerals with a higher extent of dissolution demonstrated better compressive strength after polymerization. The percentage of calcium oxide (CaO), potassium oxide (K_2O), the molar ratio of Si-Al in the source material, the type of alkali and the molar ratio of Si/Al in the solution during dissolution had significant effect on the compressive strength.

Swanepoel and Strydom (2002) conducted a study on geopolymers produced by mixing fly ash, kaolinite, sodium silica solution, NaOH and water. Both the curing time and the curing temperature affected the compressive strength, and the optimum strength occurred when specimens were cured at 60°C for a period of 48 hours.

van Jaarsveld, van Deventer and Lukey (2002) studied the interrelationship of certain parameters that affected the properties of fly ash-based geopolymer. They reported that the properties of geopolymer were influenced by the incomplete dissolution of the materials involved in geopolymerization. The water content, curing time and curing temperature affected the properties of geopolymer; specifically the curing condition and calcining temperature influenced the compressive strength. When the samples were cured at 70°C for 24 hours a substantial increase in the compressive strength was observed. Curing for a longer period of time reduced the compressive strength.

Djwantoro Hardjito, Steenie E. Wallah, Dody M. J. Sumajouw, and B. Vijaya Rangan (2004) This paper presented the development of geopolymer concrete. The binder in this concrete, the geopolymer paste, is formed by activating by-product materials, such as low-calcium (Class F) fly ash, that are rich in silicon and aluminum. In the experimental work, the fly ash from a local power generation plant was used as the source material. A combination of sodium silicate solution and sodium hydroxide

solution was used as the activator. The geopolymer paste binds the loose coarse and fine aggregates

Hardjito and B. V. Rangan (2005), Wallah and B. V. Rangan (2006) This paper describes heat-cured low-calcium fly ash-based geopolymer concrete possesses high compressive strength, undergoes very little drying shrinkage and moderately low creep, shows excellent resistance to sulphate attack, and reveals good acid resistance

D.M.J Sumajouw, D. Hardjito, S.E Wallah, B.V. Rangan(2007) investigated the results of experimental study and analysis on the behaviour and strength of reinforced geopolymer concrete slender columns. The experimental work involved testing of twelve columns under axial load and uniaxial bending in single curvature mode.

D.S. Perera, O.Uchida, E.R. Vance, K. S. Finnie (2007) studied the curing at ambient and controlled relative humidity (RH) with mild heating (40-60oC) of a metakaolinite- based geopolymer of molar ratios Si/Al and Na/Al of 2 and 1 respectively

Divya Khale, Rubina Chaudhary (2007) Investigated the mechanism of geopolymerization and factors influencing its development. And demonstrates that certain mix compositions and reaction conditions such as Al₂O₃/SiO₂, alkali concentration, curing temperature with curing time, water/solid ratio and pH significantly influences the formation and properties of a geopolymer. It is utilized to manufacture precast structures and non-structural elements, concrete pavements, concrete products and immobilization of toxic metal bearing waste that are resistant to heat and aggressive environment. Geopolymers gain 70% of the final strength in first 3–4 h of curing

Radhakrishna, A.Shashishankar, B.C. Udayashankar (2008) studied the technology of making compressed geopolymer blocks with Class F fly ash. The experimental data generated is analysed and phenomenological is advanced to arrive at the combinations of the ingredients to produce geopolymer meeting the compressive strength required at eth specified age irrespective of the molarity of the activator solution, age and aggregate used.

MATERIAL PROPERTIES



CHAPTER 3

MATERIAL PROPERTIES

3.1 MATERIALS USED

- Fly ash used in this study is (class F) dry fly ash from Mettur thermal power station(MTPS) as per IS 1489 (Part 1) – 1991
- Locally available river sand of fineness modulus of 2.67 was used as fine aggregate
- Crushed blue granite as per IS:383-1970 passing through 20mm sieve and retained on 10 mm sieve was used as coarse aggregate
- Locally available sodium silicate solution and sodium hydroxide pellets
- Potable water as per IS:456-2000 was used for the concrete preparation

3.1.1 Fly ash

Fly ash is a by-product of the combustion of pulverized coal in thermal power plants. Fly ash particles are typically spherical, ranging in diameter from <1 mm up to 150 μ m. The types and relative amounts of incombustible matter in the coal used determine the chemical composition of fly ash. More than 85% of most fly ash comprises chemical compounds and glasses formed from the elements silicon, aluminium, iron, calcium and magnesium. Generally, fly ash from the combustion of sub bituminous coals contains more calcium and less iron than fly ash from bituminous coal. The color of fly ash ranges from almost cream to dark grey depending upon the proportion of unburned carbon present. Hence it has almost same colour of the cement. Class F fly ash has pozzolonic properties only. Fly ash has been used in the past to partially replace Portland cement to produce concretes. An important achievement in this regard is the development of high volume fly ash (HVFA) concrete that utilizes up to 60 percent of fly ash, and yet possesses excellent mechanical properties with enhanced durability performance. The test results show that HVFA concrete is more durable than Portland cement concrete

(Malhotra 2002). Recently, a research group at Montana State University in the USA has demonstrated through field trials of using 100% high-calcium (ASTM Class C) fly ash to replace Portland cement to make concrete. Ready mix concrete equipment was used to produce the fly ash concrete on a large scale. The field trials showed that the fresh concrete can be easily mixed, transported, discharge, placed, and finished (Cross et al 2005). In this study, the low-calcium (ASTM Class F) dry fly ash obtained from Mettur thermal power station was used as the base material.

The specific gravity varies from 1.9 to 2.4. The specific surface area was found to be $320\text{m}^2/\text{kg}$ and they are mostly glassy hollow spherical particles. Bulk density of dry fly ash was approximately 800 kg/m^3 . The fineness modules of fly ash were $357\text{ m}^2/\text{kg}$. The chemical composition details of fly ash as per the supplier are shown in the Table 3.1

Table 3.1 Chemical composition of Fly ash

constituent	Percentage (%)
SiO ₂	54.5
Al ₂ O ₃	28.2
MgO	1.2
SO ₃	0.3
Autoclave expansion	0.04
Loss of ignition	2.3

The reactivity of the pozzolanic material with hydrated lime was conducted as per IS: 1727-1967 and the specimen of size was used. The moulds for 50mm cube specimens should be metal not attacked by lime pozzolanic mortar. The interior face of the specimen moulds was thinly covered with mineral oil and the moulds was then placed on the plane, non-material used for the standard test mortar was lime; pozzolanic: standard sand in proportion of 1; 2M: 9 by weight, blended intimately.

Where,

$M = \frac{\text{Specific gravity of pozzolana}}{\text{Specific gravity of lime}}$

Specific gravity of lime

With the dry material as specified above trial mortars with different percentage of water until specified flow was obtained. The materials for each batch of moulds were mixed separately using the quantities of dry materials conforming to the proportions obtained and the quantity of water as determined from the flow table test. Mixing of mortar was done mechanically. The prepared mortar was placed in the 50mm cube mould in a layer of about 25mm thickness and was tamped 25 times with the tamping rod. The surface of the specimen in the mould was covered with a smooth and greased glass plate with the cover plates under wet gunny bags for 48 hours the specimens were removed and cured at 90 to 100 percent relative humidity at $50 \pm 2^\circ\text{C}$ for a period of 8 days. The cured specimen from the humidity chamber was tested for compressive strength and the value was found to be 4MPa.

3.1.2 Alkaline solution

A combination of sodium silicate solution and sodium hydroxide solution was used to react with the aluminium and the silica in the fly ash. Sodium based solutions were chosen because they were cheaper than Potassium-based solutions. The sodium hydroxide (NaOH) solution was prepared by dissolving either the flakes or the pellets in water. The mass of NaOH solids in a solution varied depending on the concentration of the solution expressed in terms of Molar M. Sodium silicate solution obtained from the soap industry was used. The chemical composition of sodium silicate solution was purity of Sodium hydroxide (15.01%), purity of sodium meta silicate (59.38%). The other characteristic of the sodium silicate solution were density=1.77g/cc, solid content=69.33%, and P^H value=12.07. The test report of sodium silicate solution was given in Appendix D. The composition of alkaline solution is shown in Table 3.2

Table 3.2 Composition of alkaline solution

sodium silicate solution	
Sodium silicate solution	43.6%
Distilled water	56.4%
sodium hydroxide solution	
Sodium hydroxide flakes	26.8%
Distilled water	73.2%
alkaline solution	
Sodium hydroxide solution	26.8%
Sodium silicate solution	73.2%

3.1.3 Aggregates

Aggregates are the inert particles that are bound together by the cementing agent to form a mortar or a concrete. The boundary size definition of fine aggregate is one that passes a 4.75 mm sieve and retained on 300micron sieve. Coarse aggregate particles are those that are retained on 4.75 mm sieve. Coarse aggregates are obtained from gravel or crushed stone, blast furnace slag or recycled aggregate. Fine aggregates are derived from the same sources except that in place of gravel, naturally occurring sand is used. All aggregates should be composed of hard particles and free of injurious amounts of clay, loam and vegetable matter.

3.1.3.1 Tests on fine aggregate

Fine aggregate used for concrete was well graded locally available river sand passing through 4.75mm and retained on 300 micron, to achieve minimum void ratio and the properties of fine aggregates like fine modulus. The physical properties like fineness modulus, specific gravity, Bulk density were studied as per IS; 383-1978, and the obtained results were as shown in Table 3.3

3.1.3.2 Tests on coarse aggregate

Locally available blue granite was used. Crushed granite stones of size passing through 20mm sieve and retained on 4.75 mm sieve as per IS: 383-1970 was used for experimental purposes. Tests such as fineness modulus, specific gravity, bulk density, aggregate impact value and aggregate crushing values were performed as per IS: 2386-1963 and the results are shown in Table 3.4. The aggregate crushing and impact values were found to be within in the limits i.e. the percentage of those values were less than the 45 %. The aggregates were found to be good sounding and angular in shape. It's well fit to be used in concrete.

Table 3.3 Properties of fine aggregates

TEST	RESULT OBTAINED	As per IS:383-1978
Fineness modulus	2.6	Medium sand
Specific gravity	2.67	2.55 minimum
Bulk density kg/m ³	1578.17	-

Table 3.4 Properties of coarse aggregate

Test	Result obtained	As per IS: 383 - 1978
Fineness modulus	6.2	5 to 7
Specific gravity	2.66	2.6 minimum
Bulk density kg/m ³	161	-
Impact value	32.5	< 45 %
Crushing value	34.5	< 45 %

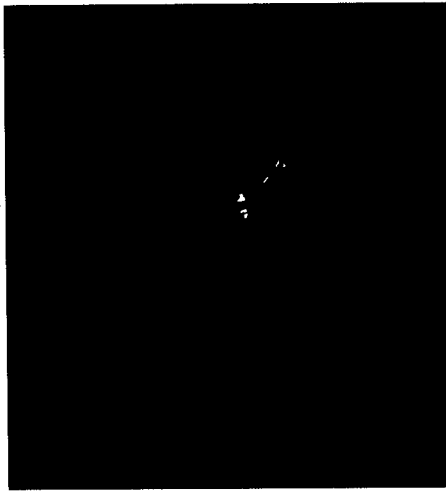


Figure 3.1 Class F fly ash



Figure 3.2 Fine Aggregates



Figure 3.3 Coarse Aggregates



Figure 3.4 Sodium Hydroxide pellets

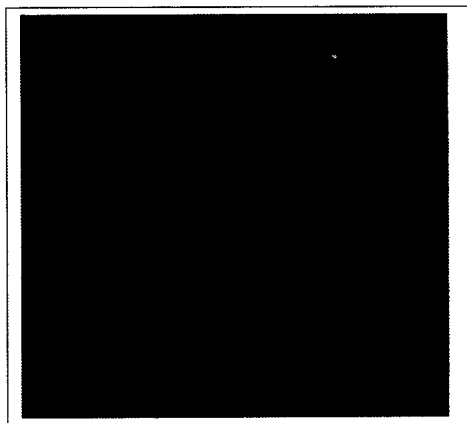


Figure 3.5 Sodium silicate Solution

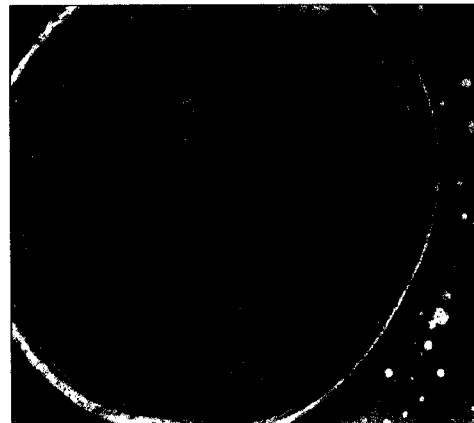


Figure 3.6 Alkaline solution

3.2 MIXTURE PROPORTION OF GEOPOLYMER CONCRETE

Concrete may be considered as composed of basic separate ingredients: cement, fine aggregates, coarse aggregates and water. For geopolymer concrete, instead of cement fly ash, alkaline solution, fine aggregates and coarse aggregates are used. The requirements of concrete are complex, but the ultimate aim is to produce the most economical combination of concrete materials that will satisfy the performance requirements and applications. A concrete mix design can be proportioned from existing statistical data using the same materials, proportion and concreting conditions. When there are no existing records or they are insufficient, the concrete mixture must be determined by trial mixtures. Based on the information given above, some simple guidelines for the design of steam-cured fly ash based geopolymer concrete. The role and the influence of aggregate are considered to be the same as in the case of Portland cement concrete. The mass of combined aggregate may be taken to be between 75% and 80% of the mass of geopolymer concrete. The performance criteria of a geopolymer concrete mixture depend on the application. For simplicity, the compressive strength of hardened concrete is selected as the performance criteria. In order to meet these performance criteria, the alkaline liquid-to-fly ash ratio by mass, water-to-geopolymer solids ratio by mass, the wet-mixing time, the heat-curing temperature, and the heat-curing time are selected as parameters. With regards to alkaline liquid-to-fly ash ratio by mass, values in the range of 0.30 and 0.45 are recommended.

Mixture proportion of fly ash based geopolymer concrete with design compressive strength of 20MPa (GPC-1) and 35 MPa (GPC-2) were done. The combined aggregate may be selected to match the standard grading curves used in the design of Portland cement concrete mixtures. The combination of different size aggregates were decided on the basis of experimenting. The different sizes of aggregates used were 20mm, 16mm, 12.5mm and 10mm. To manufacture the geopolymer concrete mixture, locally available sodium silicate solution from soap industry is using. The sodium hydroxide solids (NaOH) with 97-98% purity were obtained from commercial source and the solution with a concentration of 16M is prepared. This solution comprises 26.2% of

NaOH solids and 68.6% water, by mass. The aggregate are assumed to be in saturated surface dry condition. The geopolymer concrete must be wet mixed at least for four minutes and steam cured at 75°C for 24 hours after casting. The details of geopolymer mixes are given in Table 3.5. The mix proportion of PPC concrete done according to IS 10262-1982 and given in Table 3.6.

Table 3.5 Mixture proportion of Geopolymer concrete (GPC)

Mix	GPC-1	GPC-2
Flyash (Kg/m ³)	326	326
Alkaline solution (Kg/m ³)	165	230
Fine aggregate (Kg/m ³)	443	443
20 mm aggregate (Kg/m ³)	415	415
16 mm aggregate (Kg/m ³)	415	415
12.5 aggregate (Kg/m ³)	415	415
10 mm aggregate (Kg/m ³)	415	415
Temperature of steam curing (°C)	75	75
Time of curing	24	24
Density of concrete(Kg/m ³)	2390	2462
Compressive strength(N/mm ²)	20.0	37.0

Table 3.6 Mix proportion of Portland Pozzolona cement concrete (PPC)

Cement (Kg/m ³)	378
Fine aggregate (Kg/m ³)	554
Coarse aggregate (Kg/m ³)	1227
W/C	0.5



Figure 3.7 Dry mixing of GPC

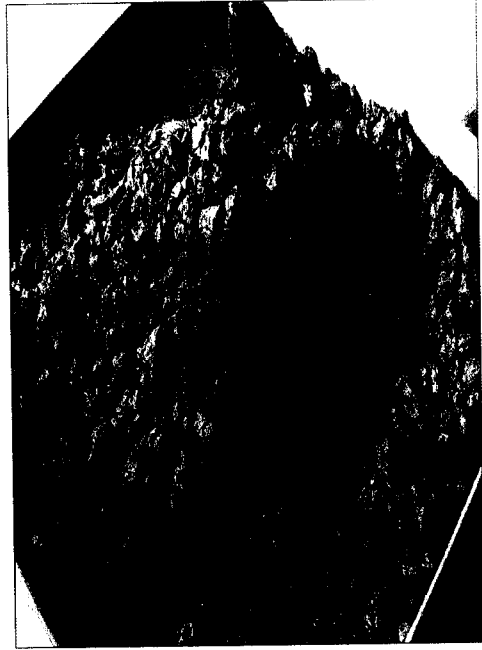


Figure 3.8 Wet mixing GPC

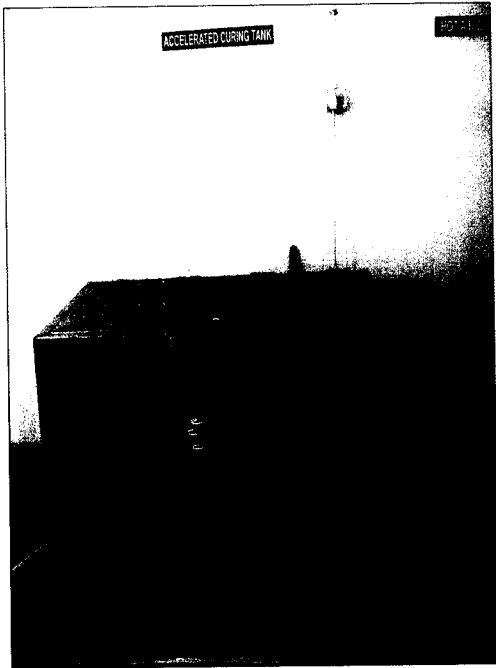


Figure 3.9 Steam Curing chamber

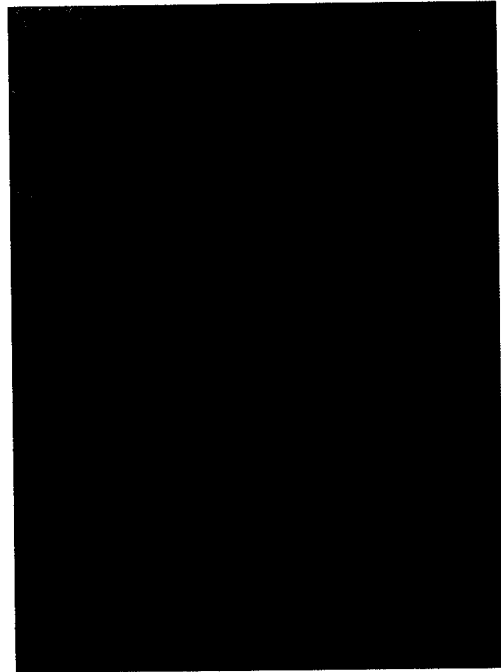


Figure 3.10 Hot air oven

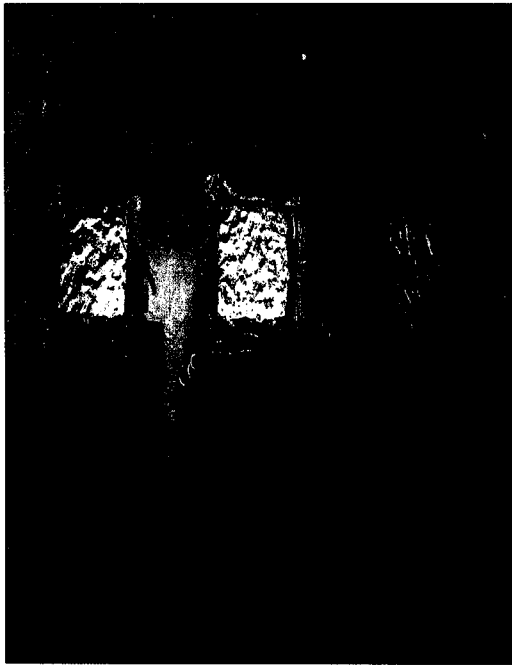


Figure 3.11 Mould with GPC

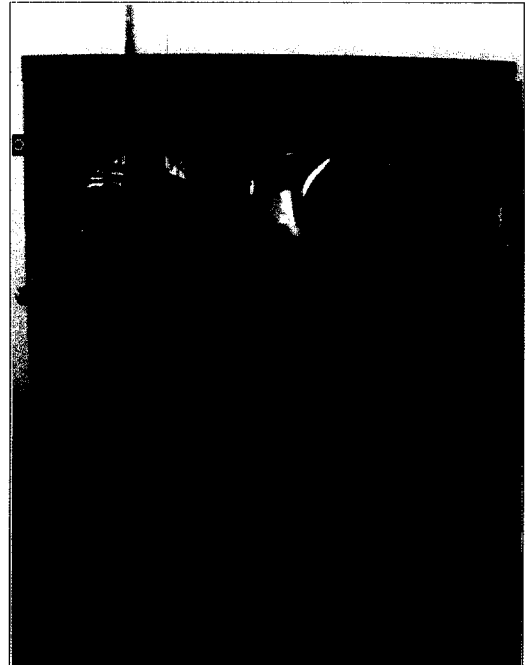


Figure 3.12 Oven curing of specimens

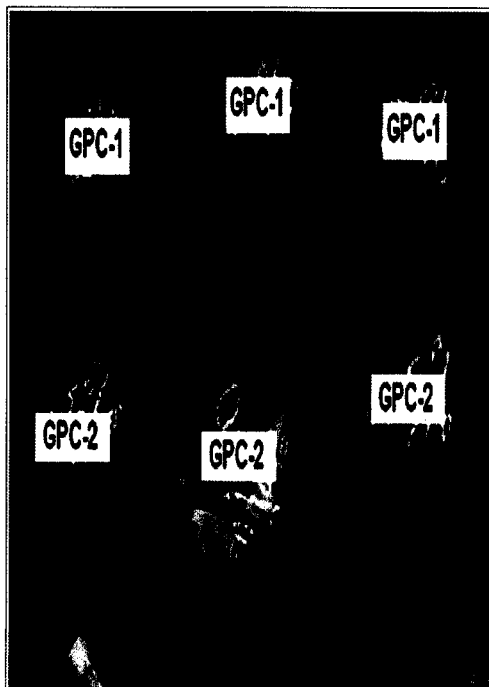


Figure 3.13 Cylinders after curing

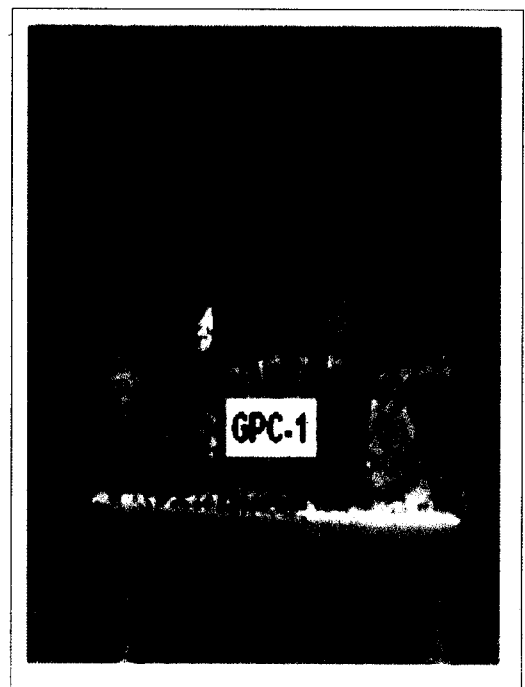


Figure 3.14 Cubes after curing (GPC-1)

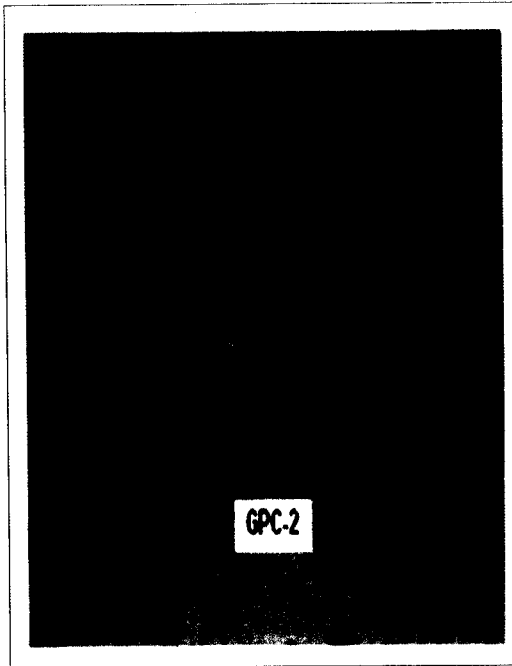


Figure 3.15 Cubes after curing (GPC-2)

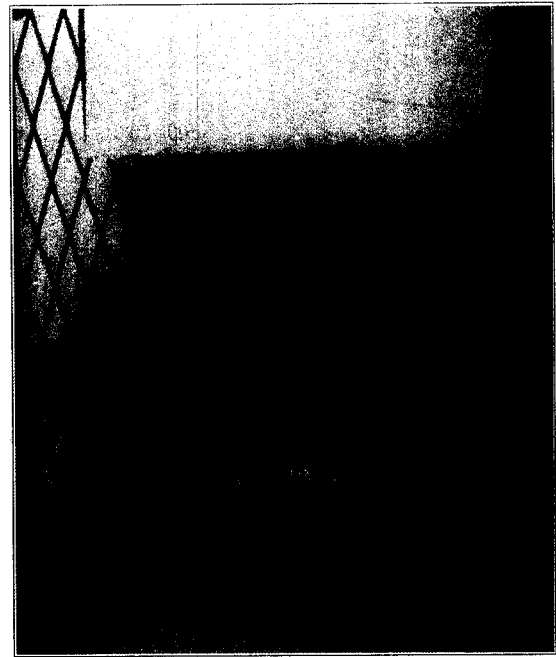


Figure 3.16 Compressive strength test

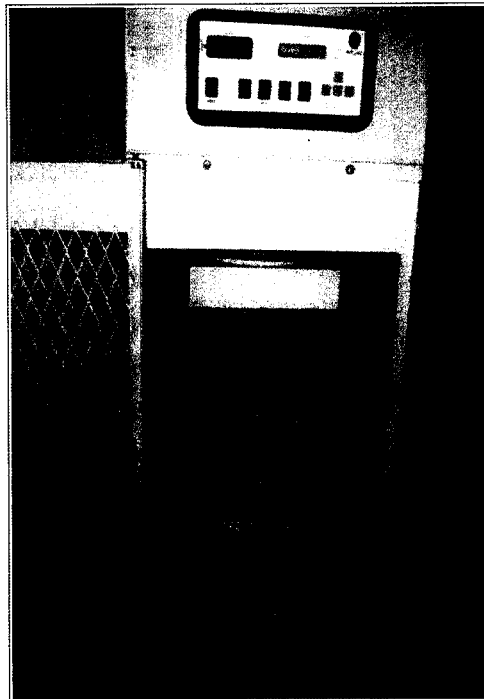


Figure 3.17 Split tensile strength test

3.3 REINFORCING BARS

Three different sizes of high yield strength deformed bars (HYSD), conforming to IS 1786-1985 were used as the longitudinal reinforcement. Samples of steel bars were tested in the laboratory. The results of these tests are given in Table 3.7 and Table 3.8

Table 3.7 Properties of steel reinforcement

Diameter of steel (mm)	Length in cm	Mass per meter run (Kg/m)	As per IS 1786-1985 Mass per meter run (Kg/m)
8	100.00	0.400	0.395
10	100.00	0.621	0.617
12	100.00	0.894	0.888

Table 3.8 Characteristics of steel reinforcement

Diameter of steel (mm)	Yield load (KN)	Yield stress* N/mm ²	Ultimate load (KN)	Ultimate stress** N/mm ²	% of elongation***
8	34.30	682.29	42.20	839.43	25.23
10	41.90	420.11	48.50	541.06	20.67
12	47.70	421.71	60.10	530.45	17.33

Note:

*Yield stress : Not less than 415 N/mm²

**Ultimate stress : Not less than 485 N/mm²

***% of elongation : Not less than 14.5 %

MAIN THEME OF PROJECT



CHAPTER 4

MAIN THEME OF THE PROJECT

4.1 INTRODUCTION

This Chapter describes the manufacture of test specimens, and presents the detail of the test program. Six reinforced concrete beams and four reinforced concrete columns were manufactured and tested. The test parameters covered a range of values encountered in practice. The sizes of test specimens were selected to suit the size of steam curing chamber available in the laboratory. The tensile reinforcement ratio was the test parameters for beam specimens. In the case of column specimens, the lateral tie spacing was the test parameter.

4.2 EXPERIMENTAL PROGRAMME

4.2.1 Beams

4.2.1.1 Geometry and reinforcement configuration

All beams were 175mm wide by 175mm deep in cross-section; they were 900mm in length and simply-supported over a span of 720mm. The beams were designed to fail in a flexural mode. Three different tensile reinforcement ratios were used. The clear cover to reinforcement was 20 mm on all faces. The geometry and reinforcement details of beams are shown in Figure 4.1 and Table 4.1

4.2.1.2 SPECIMEN MANUFACTURE AND CURING PROCESS

Figure 4.2 shows the reinforcement cages, and Figure 4.3 moulds with reinforcement. The coarse aggregates and the sand in saturated surface dry condition were first mixed with the fly ash for about three minutes. At the end of this mixing, the alkaline solutions together and the extra water were added to the dry materials and the mixing continued for another four minutes. Immediately after mixing (Figure 4.4), the fresh concrete was cast into the moulds. All beams were cast horizontally in steel moulds

in two layers. Each layer was compacted using a needle vibrator (Figure 4.5 and Figure 4.6). With each batch, three numbers of 100mm size cubes were also cast. These cubes were tested in compression on the same day as the beam tests. After casting, all specimens were kept in steam curing chamber for 24 hours. To avoid condensation over the concrete, a steel sheet was used to cover the concrete surface. After curing, the beams and the cubes were removed from the chamber and de-moulded. The specimens are again kept in steam curing chamber for another 5 hours (Figure 4.7 and Figure 4.8) shows the curing process. The test specimens (Figure 4.9) were then left in the laboratory ambient conditions until the day of testing. The laboratory temperature varied between 25°C and 35°C during that period.

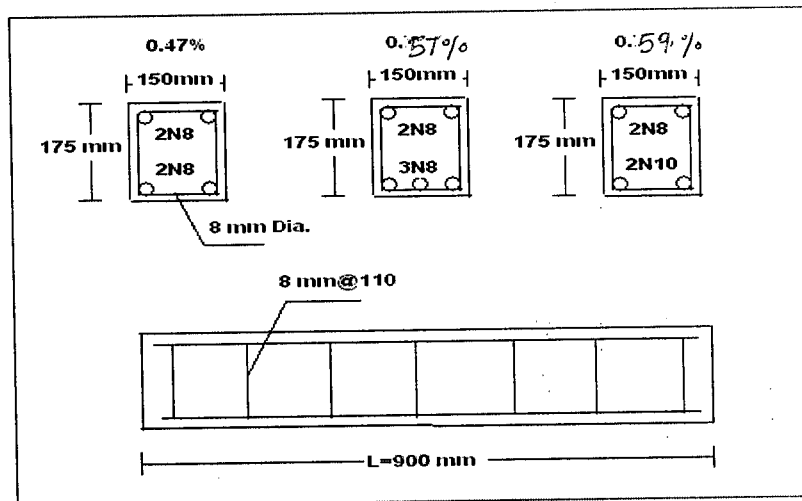


Figure 4.1 Geometry and reinforcement details

Table 4.1 Beam specimen details

Beam no.	Beam size B X D X L (mm)	Tension reinforcement no. and size	Compression reinforcement no. and size	Area of tensile steel A_{st} (mm ²)	Tensile reinforcement ratio (%)
PPC-B1	150 X175X 900	2N8	2N8	100.53	0.38
PPC-B2	150 X175X 900	3N8	2N8	150.79	0.57
PPC-B3	150 X175X 900	2N10	2N8	157.08	0.59
GPC-B1	150 X175X 900	2N8	2N8	100.53	0.38
GPC-B2	150 X175X 900	3N8	2N8	150.79	0.57
GPC-B3	150 X175X 900	2N10	2N8	157.08	0.59



Figure 4.2 Reinforcement cages

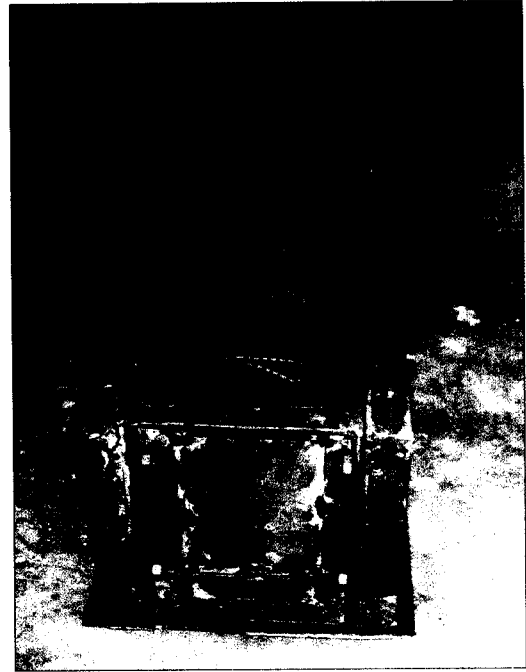


Figure 4.3 Mould with reinforcement



Figure 4.4 GPC after mixing



Figure 4.5 Compaction using needle vibrator

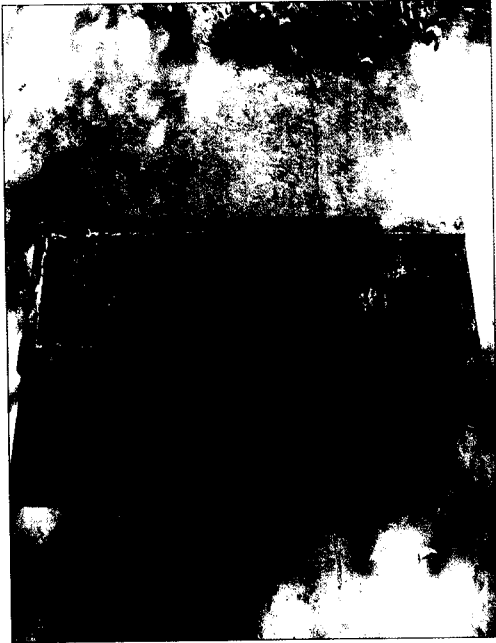


Figure 4.6 GPC in beam mould



Figure 4.7 Steam curing with mould

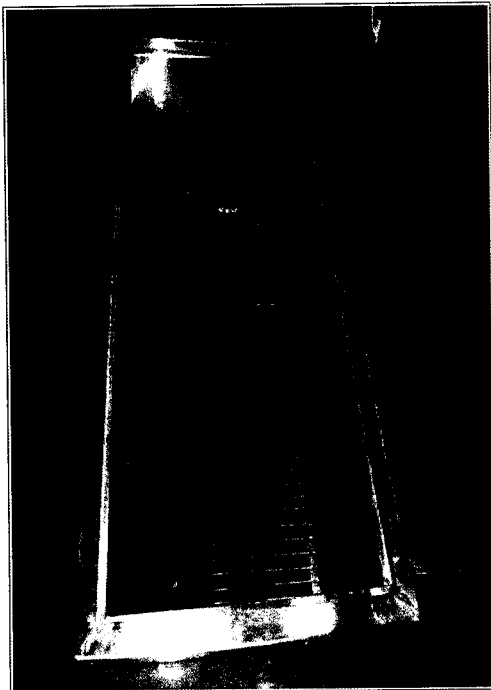


Figure 4.8 Steam curing without mould

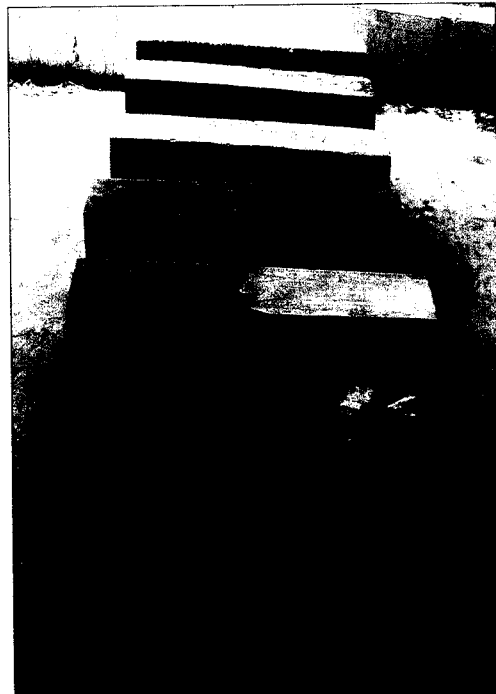


Figure 4.9 Beam specimens after finishing

4.2.1.3 Test set-up and instrumentation

The setup for the flexure tests was designed to create a constant moment region at mid-span of the beam. All beams were simply supported over a span of 720 mm and tested in a loading frame with a capacity of 300 KN. Two concentrated loads placed symmetrically over the span loaded the beams. The distance between the loads was 240 mm. The test configuration is shown in Figure 4.10. Digital data acquisition unit was used to collect the data during the test. Linear Variable Differential Transformers (LVDTs) were used to measure the deflections at selected locations along the span of the beam. All LVDTs were calibrated prior to tests. The relationship between output of the LVDTs in milli-volts (mV) and real movement in millimeters (mm) was determined to be linear.

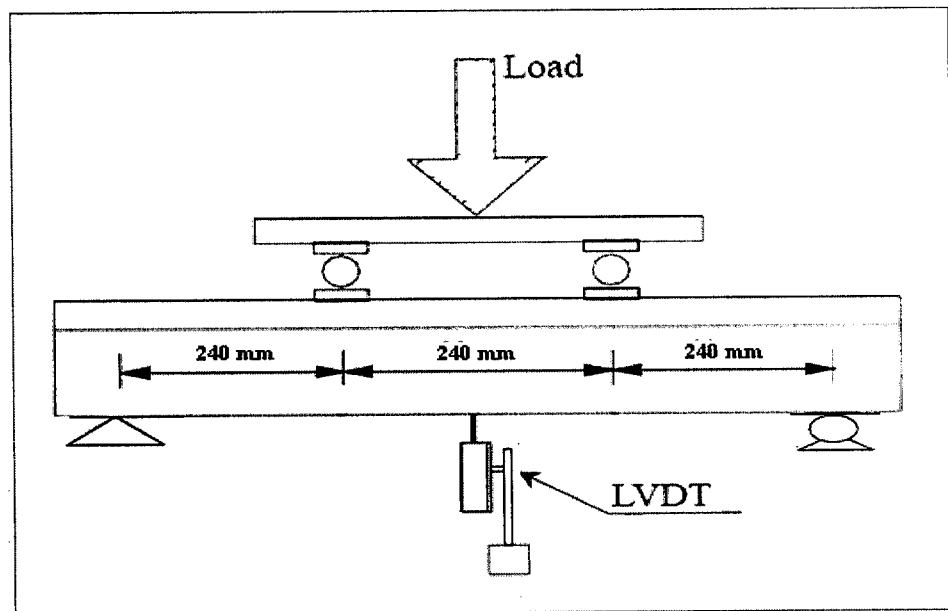


Figure 4.10 bending test of beams

4.2.1.4 Test procedure

Each beam was simply supported over a span of 720 mm and tested under third-point loading. Two point symmetrical loading was applied in most of the tests to produce

a constant moment in the mid-span region of the beams. Prior to testing, all beams were suitably instrumented for measuring mid-span deflection using a linear variable differential transducer (LVDT). The load was then applied monotonically using a load jack and a computer captured all deformation readings at preset load intervals until the beam failed. The tests started with a constant movement of the test machine crosshead of 0.1 mm/min. The tests were stopped when any of the following conditions were met: the specimens failed completely; the LVDTs at mid-span reached full scale. The second condition was met only at very large deformations. In most cases, the ultimate strains were not recorded since, as mentioned above, the LVDTs had been removed prior to failure in order to avoiding of same.

4.2.2 Columns

4.2.2.1 Geometry and reinforcement configuration

All columns were provided with column heads at the top and bottom to facilitate easy loading and to avoid local failure of concrete. The geometry and reinforcement details of beams are shown in Figure 4.11 and Table 4.2

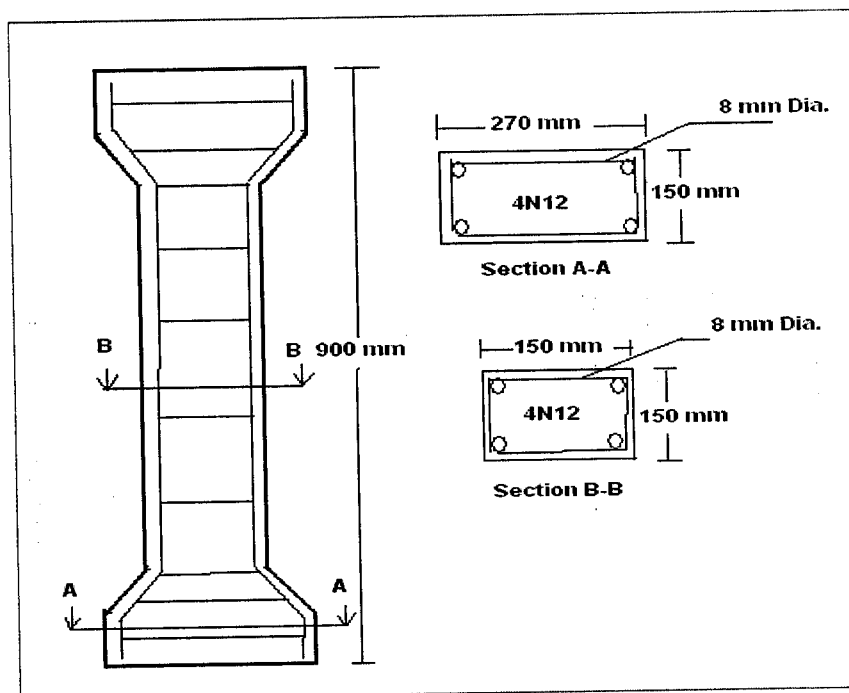


Figure 4.11 Geometry and reinforcement details column

Table 4.2 Column specimen details

Column no.	Column size (mm)	Longitudinal reinforcement	Lateral ties @
PPC-C1	150X150X900	4N12	120
PPC-C2	150X150X900	4N12	100
GPC-C1	150X150X900	4N12	120
GPC-C2	150X150X900	4N12	100

4.2.2.2 Specimen manufacture and curing process

Figure 4.12 shows the reinforcement cages, and Figure 4.13 moulds with reinforcement. The coarse aggregates and sand were in saturated surface dry condition. The aggregates and the dry fly ash were first mixed for about three minutes. While mixing, the alkaline solutions and the extra water were mixed together and added to the solid particles. The mixing of the wet mixture continued for another four minutes. The fresh concrete was cast into the moulds immediately after mixing (Figure 4.14). All columns were cast horizontally in wooden moulds in two layers. Each layer was compacted using needle vibrator (Figure 4.15 and Figure 4.16). After casting, all specimens were kept in steam curing chamber for 24 hours. To avoid condensation over the concrete, a steel sheet was used to cover the concrete surface. After curing, the beams and the cubes were removed from the chamber and de-moulded. The specimens are again kept in steam curing chamber for another 5 hours. Figure 4.17 and Figure 4.18 shows the curing process. The test specimens were then left in the laboratory ambient conditions until the day of testing (Figure 4.19). The laboratory temperature varied between 25°C and 35°C during that period.

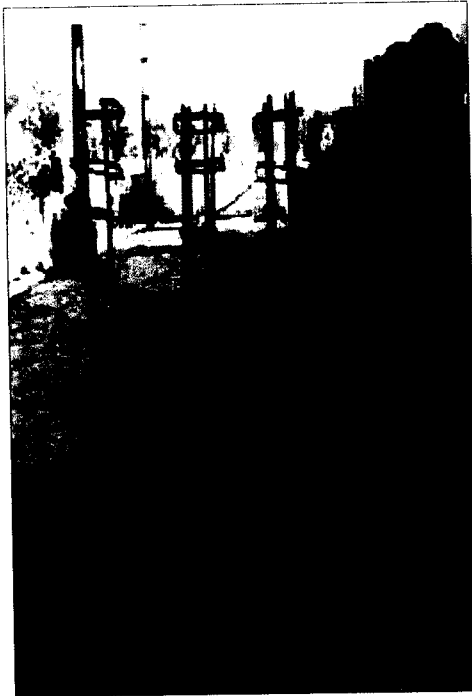


Figure 4.12 Reinforcement cages

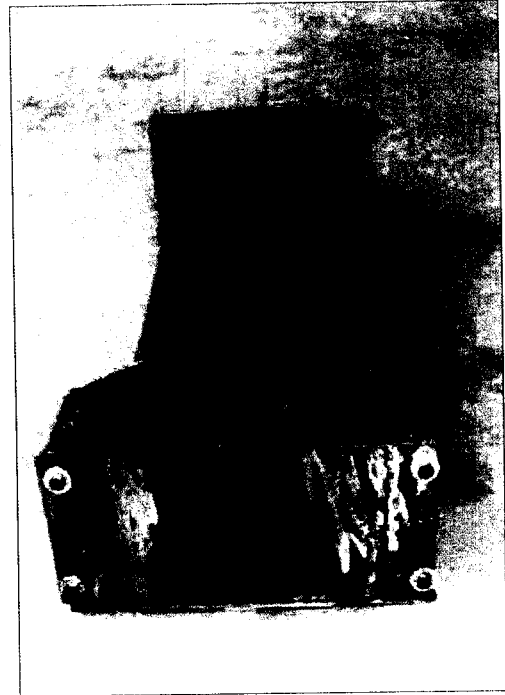


Figure 4.13 Mould with reinforcement



Figure 4.14 GPC after mixing



Figure 4.15 Compaction using needle vibrator



Figure 4.16 GPC in column mould

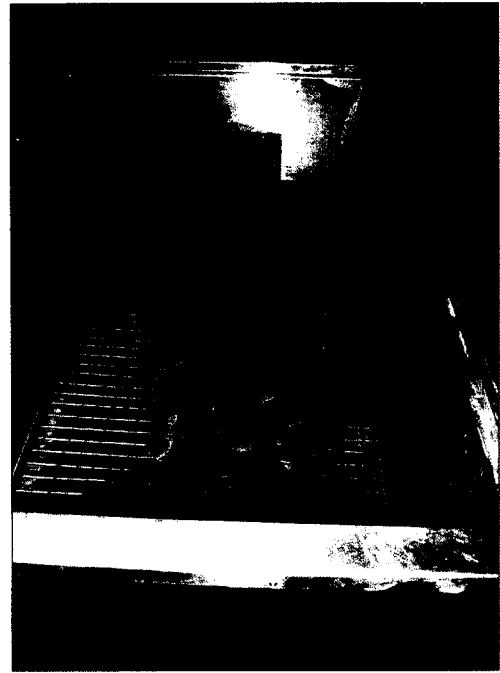


Figure 4.17 Steam curing with column mould



Figure 4.18 Steam curing without mould



Figure 4.19 Column specimens after finishing

4.2.2.3 Test set-up and instrumentation

The column specimens were tested in a frame that was specifically designed for this research (Figure 4.20). Linear Variable Differential Transformers (LVDTs) were used to measure the longitudinal shortening of column. LVDTs were calibrated prior to tests. The relationship between output of the LVDTs in milli-volts (mV) and real movement in millimeters (mm) was determined to be linear.

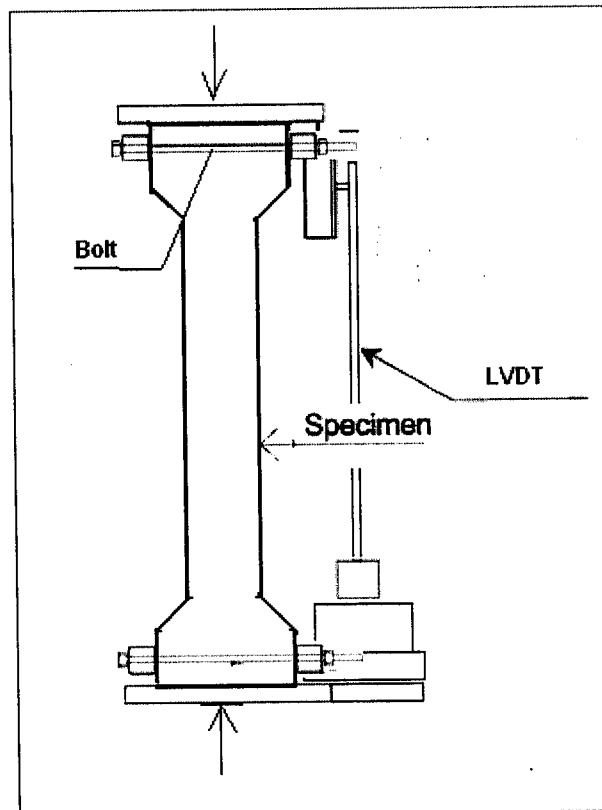


Figure 4.20 Test configuration column

4.2.2.4 Test procedure

Tests were done in a 50 KN testing machine using load jack. A preload was applied to the test specimen and was held while all of the bolts were tightened. After the specimen had been checked to ensure proper positioning, it was unloaded, and zero readings were recorded. The tests started with a constant movement of the test machine crosshead of 0.1 mm/min. The tests were stopped when any of the following conditions

were met: the specimens failed completely; the LVDTs on the compression side reached full scale. The second condition was met only at very large deformations. In most cases, the ultimate strains were not recorded since, as mentioned above, the LVDTs had been removed prior to failure in order to avoid damaging of same.

*PRESNTATION AND
DISCUSSION OF RESULTS*

CHAPTER 5

PRESENTATION AND DISCUSSION OF TEST RESULTS

5.1 TEST RESULTS ON FRESH CONCRETE

The compacting factor test is one of the most efficient tests for measuring the workability of concrete as per IS: 1199-1959. It is the most precise, sensitive and particularly useful for concrete mixes of very low workability as are normally used, when concrete is to be compacted by vibration and GPC is handled for 60-100 minutes. The workability of fresh geopolymer concrete is expected to be moderate. If needed, commercially available super plasticizer of about 1.5% of mass of fly ash, i.e. $408 \times (1.5/100) = 6 \text{ Kg/m}^3$ may be added to the mixture to facilitate ease of placement of fresh concrete. Water content and Super Plasticizer play an important role with regard to Workability Concrete. The results obtained from the compaction factor test for mixes (GPC-1, GPC-2) are shown in the Table 5.1

Table 5.1 Results of compaction factor values for GPC

Test	GPC-1	GPC-2
C.F	0.73	0.86

5.2 TEST RESULTS ON HARDENED CONCRETE

The hardened properties of concrete like compressive strength test and split tensile test for the concrete mixes were conducted as per IS: 516-1959, IS: 5816-1999 and ASTM standards.

5.2.1 Compressive Strength

The compressive strength of GPC was conducted on the cubes of size 100mm were tested as per IS 516 –1959 specifications and the experimental setup as shown in Figure 3.16. The unit weights of the specimens were also determined at the same time. The cubes were tested for compressive strength at the age of seventh day after

casting. For these numerous specimens made from Mixtures GPC-1 & GPC-2 are cured at 75°C for 24 hours after casting. Then the cubes are de moulded and re-cured in steam chamber for a period of 5 hours, 3 specimens were tested at different time of curing and the of the test result are shown in the Table 5.2. 3 cubes from GPC-1 mix are casting and cured in steam chamber and hot air oven. Comparison of the test results are shown in Table 5.3. The steam cured concrete cubes showing 10% less compressive strength than oven cured concrete cubes.

Table 5.2 Test result of compressive strength test of GPC

Mix designation	Time of curing	Load applied (KN)	Compressive strength (N/mm ²)
GPC-1	15 hours	150	15.0
	18 hours	180	18.0
	24 hours	200	20.0
GPC-2	15 hours	220	22.0
	18 hours	290	29.0
	24 hours	370	37.0

Table 5.3 Comparison between steam curing and oven curing

Mix designation	Time of curing	Type of curing	Load applied (KN)	Average Compressive strength (N/mm ²)
GPC-1	24 hours	Oven curing	194	20.0
			202	
			204	
	24 hours	Steam curing	186	18.0
			176	
			178	

5.2.2 Split Tensile Strength

Spilt tensile strength test is an indirect method of finding the tensile strength of concrete. It is easy to perform and gives more uniform strength than tension test. The specimen is loaded horizontally between the loading surfaces of the compression testing machine and is loaded until the failure of the cylinder. Spilt tensile test was conducted at the age of seventh day after casting. For these numerous specimens made from Mixtures GPC-1 and GPC-2 are cured at 75°C for 24 hours after casting. Then the cubes are de moulded and re-cured in steam chamber for a period of 5 hours, 3 specimens were tested and the average values of the test result are shown in the Table 5.4. The experimental setup as shown in Figure 3.17.

Table 5.4 Test result of split tensile strength test of

Mix designation	Time of curing	Load applied (KN)	Split tensile strength (N/mm ²)
GPC-1	15 hours	119	1.68
	18 hours	135	1.91
	24 hours	156	2.21
GPC-2	15 hours	121	1.71
	18 hours	142	2.01
	24 hours	163	2.31

5.3 BEAMS

5.3.1 General Observations

In a simply-supported beam subjected to third-point loading, the middle third of the span bears a constant maximum bending moment and zero shear force, while the remaining adjoining spans are subjected to maximum shear force and varying bending moment. Collapse of beams may occur through flexural failure caused by the crushing of the concrete in compression and/or the fracture of the tension reinforcement, through diagonal tension failure of the concrete, or through shear-bond failure. The mode of failure, however, depends on the amounts of tension and shear reinforcement, the strength of the concrete, and the shear span-to-effective-depth ratio. All beams showed typical structural behaviour in flexure. No horizontal cracks were observed at the level of the reinforcement, which indicated that there were no occurrences of bond failure.

Vertical flexural cracks were observed in the constant-moment region and final failure occurred due to crushing of the compression concrete with significant amount of ultimate deflection. Since all beams were under-reinforced, yielding of the tensile reinforcement occurred before crushing of the concrete cover in the pure bending zone. When maximum load was reached, the concrete cover on the compression zone started to spall. Eventually, crushing of the concrete cover occurred during failure.

5.3.2 Flexural Capacity

Hardened concrete has a high compressive strength; its tensile strength is very low. The introduction of steel reinforcement bars in the tension zone of the beam enables the applied load to be increased considerably until the beam fails by yielding of the steel in the bottom in tension and crushing of the concrete in the top fibers in compression. The neutral axis at failure has moved to a position nearer the top of the beam. Since the strain in the material is directly proportional to the distance from the neutral axis, flexural tensile cracking will begin at the extreme bottom fibers and extend towards the neutral axis. The inverted 'V' shape is characteristic of flexural cracking in concrete. It was noticed that the first crack always appears close to the mid-span of the beam. The cracks forming on the surface of the beams were mostly vertical, suggesting failure in flexure. The presence of several short-spaced cracks within the constant moment span in most of the beams generally indicates good bond between the reinforcement and its surrounding concrete. A comparison between the experimental ultimate moments (M_{ult}) and the theoretical design moments are shown in Table 5.5. The theoretical design moment (M_{des}) of the beams was predicted using the rectangular stress block analysis as recommended by IS 456:2000. Comparison of ultimate load of geopolymer and conventional concrete beams are given in Table 5.6 and Figure 5.1 respectively

Table 5.5 Comparison between experimental and theoretical Ultimate moment of GPC beams

Beam no.	(1) Experimental Ultimate moment M_{ult} (KNm)	(2) Theoretical Design moment M_{tdes} (KNm)	Capacity ratio (1)/(2)
PPC-B1	8.86	4.97	1.78
PPC-B2	9.75	7.09	1.38
PPC-B3	13.52	7.33	1.84
GPC-B1	7.89	4.97	1.59
GPC-B2	8.25	7.09	1.16
GPC-B3	12.52	7.33	1.71

Table 5.6 Percentage reduction in Ultimate load carrying capacity of GPC beams

Beam no.	Ultimate load (KN)	% Reduction in ultimate load
PPC-B1	59.05	11.09
GPC-B1	52.52	
PPC-B2	65	15.38
GPC-B2	55	
PPC-B3	90.13	7.38
GPC-B3	83.47	

These test trends show that, as expected, the flexural capacity of beam increased significantly with the increase in the tensile reinforcement ratio. The ultimate load carrying capacity of geopolymer concrete beams is 7-15 % less than that of Portland pozzolonic cement concrete beams, because compressive strength of steam curing geopolymer concrete showing 10 % less strength than oven curing geopolymer concrete.

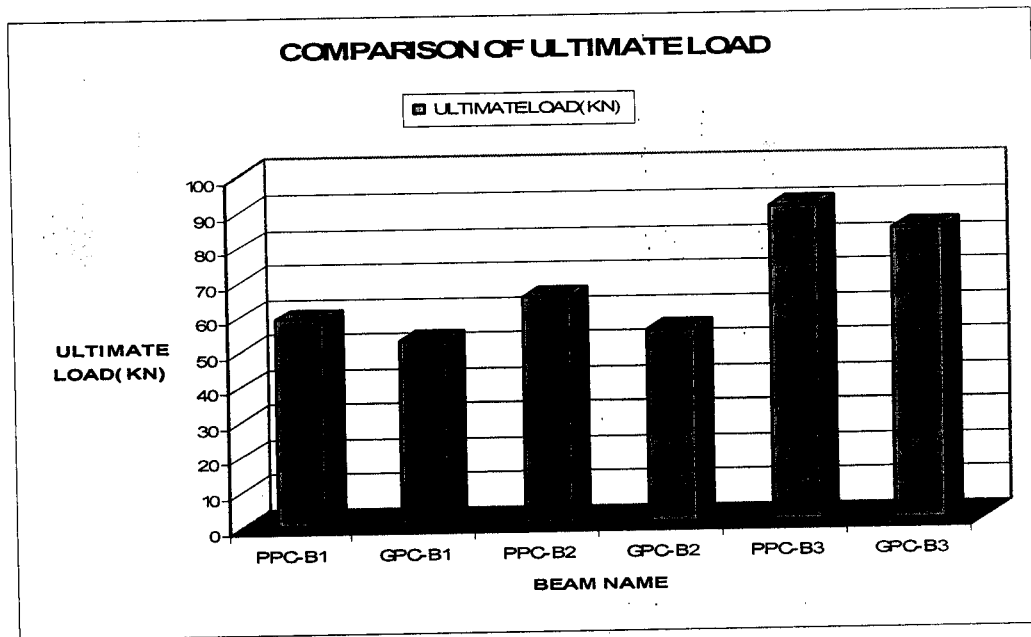


Figure 5.1 Graphical comparison of ultimate moment of GPC and PPC

5.3.3 Cracking Moment

Concrete in the extreme tension fiber of a beam section is expected to crack when the stress reaches the value of modulus of rupture f_{cr} . At this stage, the maximum strain in compression and tension are of a low order. Hence, assuming a linear stress-strain relation for concrete in both tension and compression, with same elastic modulus, the theoretical cracking moment $M_{cr (theo)}$ of the beam is determined using the formula as recommended by ACI 318 (Eq.5)

$$M_{cr (theo)} = f_{cr} I_T / Y_t \quad (5)$$

Where f_{cr} = Modulus of rupture

I_T = Second moment of area of the transformed concrete section with reinforcement with reference to NA

Y_t = Distance between the neutral axis and the extreme tension fiber

The load at which the first flexural crack was visibly observed was recorded. From these test data, the experimental cracking moment $M_{cr (exp)}$ were determined. The cracking characteristics of beams are illustrated in Table 5.7

Table 5.7 Cracking characteristics of beams

Beam no.	(1) Experimental Cracking moment $M_{cr (exp)}$ KNm	(2) Theoretical cracking moment $M_{cr (theo)}$ KNm	(1)/(2)
PPC-B1	3.96	2.64	1.5
PPC-B2	3	1.79	1.68
PPC-B3	4.93	2.78	1.77
GPC-B1	2.97	2.64	1.13
GPC-B2	2.25	1.79	1.23
GPC-B3	2.92	2.78	1.05

5.3.4 Deflection

The specimens were tested under monotonically increasing load until failure. As the load increased, beam started to deflect and flexural cracks developed along the span of the beams. Eventually, all beams failed in a typical flexure mode. Figure 5.2 shows an idealized load-deflection curve at mid-span of beams. The progressive increase of deflection at mid-span is shown as a function of increasing load. The load-deflection curves indicate distinct events that were taking place during the test. These events are identified as first cracking (A), yield of the tensile reinforcement (B), crushing of concrete at the compression face associated with spalling of concrete cover (C), a slight drop in the load following the ultimate load (C'), and disintegration of the compression zone concrete as a consequence of buckling of the longitudinal steel in the compression zone (D). These features are typical of flexure behaviour of reinforced concrete beams (Warner et al 1998).



Figure 5.3 Crack pattern and failure mode of beam PPC-B1

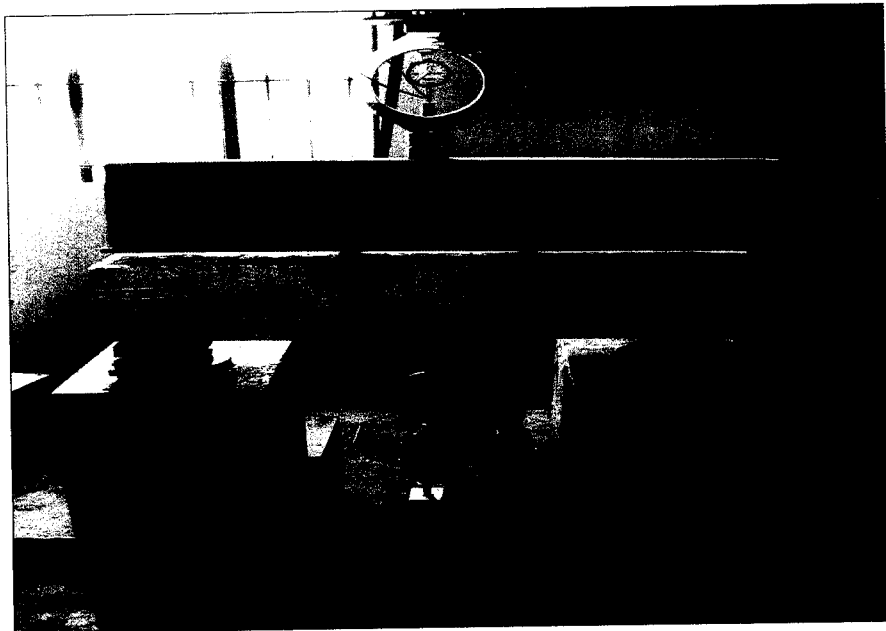


Figure 5.4 Crack pattern and failure mode of beam PPC-B2

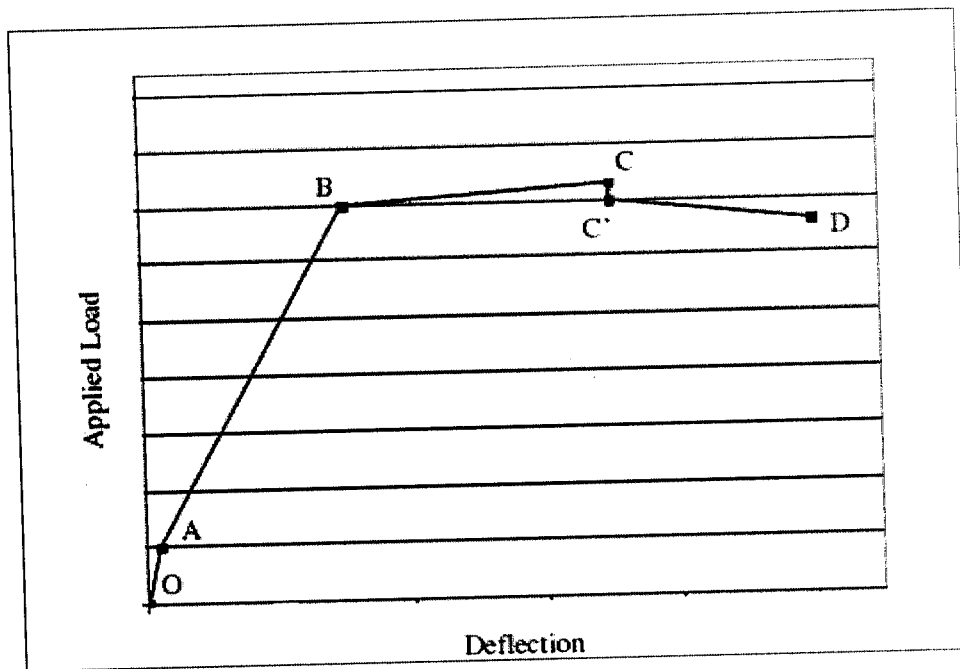


Figure 5.2 Idealised load-deflection curve

All beams behaved in a similar manner, although the distinct events shown in Figure 5.2 were not clearly identified in all cases. All test beams were designed as under reinforced beams; therefore the tensile steel must have reached its yield strength before failure. The load - deflection values for each beam given in Appendix A. The crack patterns and failure mode of several test beams are shown in Figure 5.3 to Figure 5.6. The distinct events indicated in Figure 5.2 are marked on the load-deflection curves of each beam and given in Appendix B. The graphical comparison of load-deflection curve for GPC and PPC beams are given in Figure 5.7 to Figure 5.9.

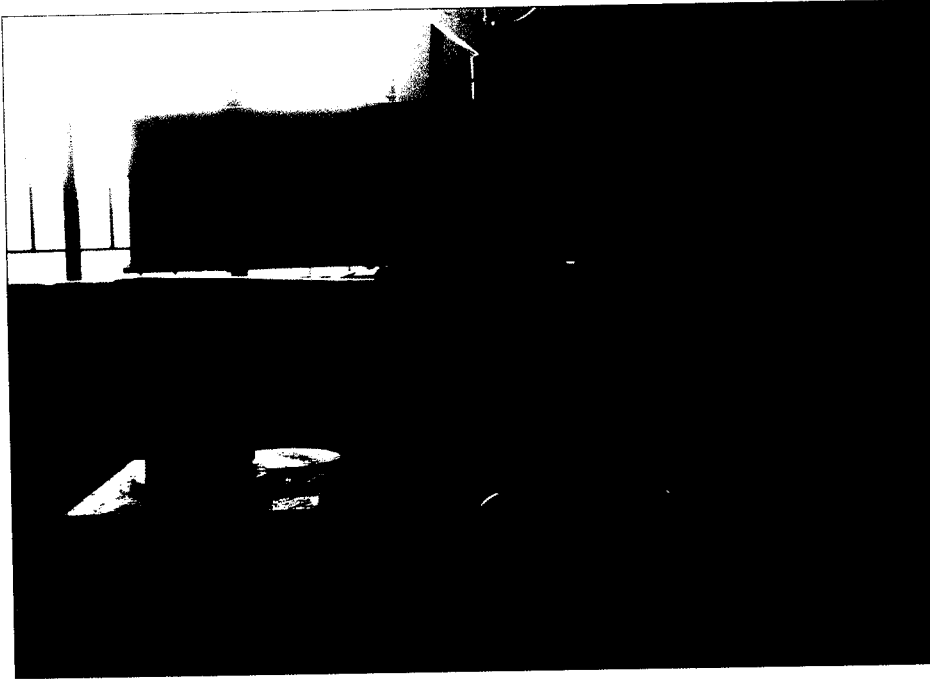


Figure 5.5 Crack pattern and failure mode of beam GPC-B1

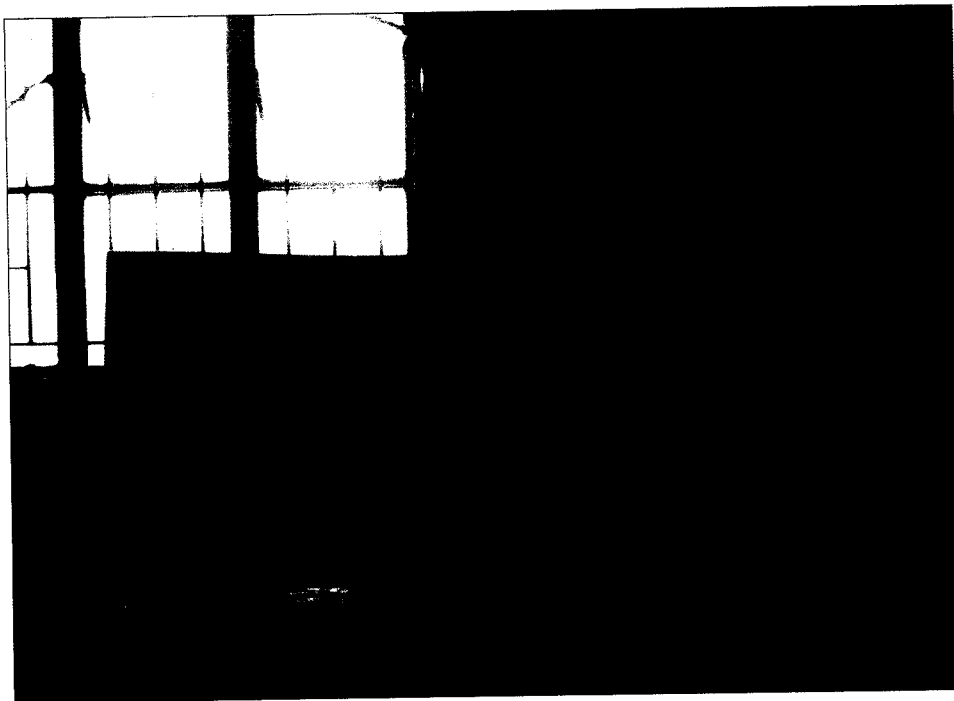


Figure 5.6 Crack pattern and failure mode of beam GPC-B2

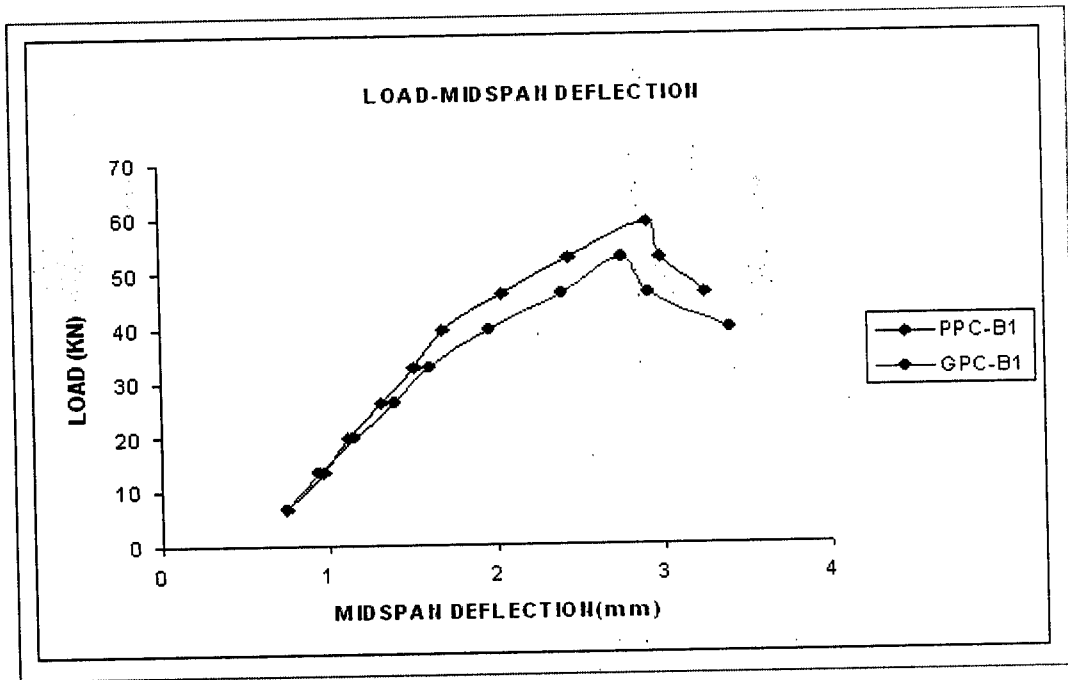


Figure 5.7 Load versus Mid-span deflection of beams PPC-B1 and GPC-B1

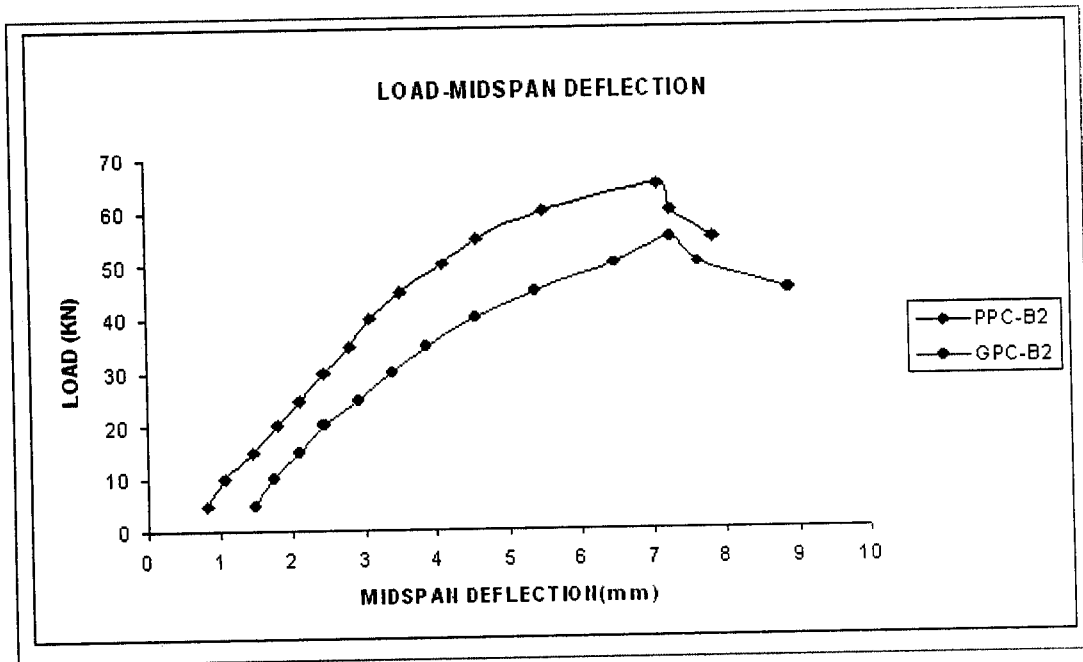


Figure 5.8 Load versus Mid-span deflection of beams PPC-B2 and GPC-B2

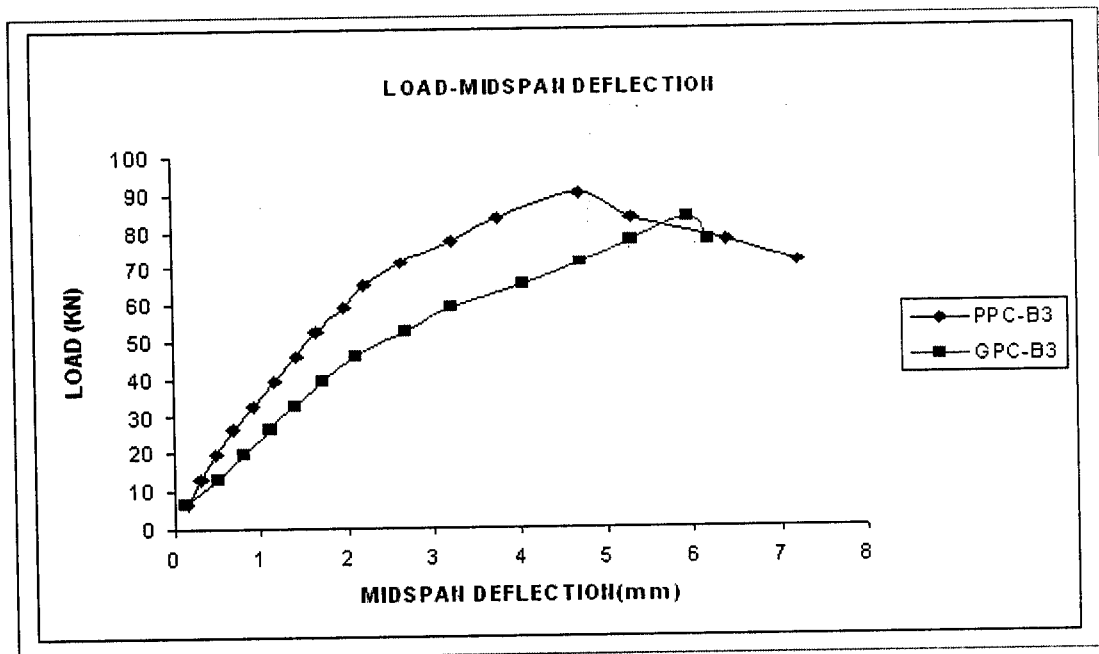


Figure 5.9 Load versus Mid-span deflection of beams PPC-B3 and GPC-B3

5.3.5 Ductility

The ductility of reinforced concrete structures is also of paramount importance because any member should be capable of undergoing large deflections at near maximum load carrying capacity, providing ample warning to the imminence of failure. In this study, the displacement ductility was investigated. Table 5.8 shows the ductility of the tested geopolymer concrete beams. The displacement ductility ratio is taken in terms of $\mu = \Delta_u / \Delta_y$, which is the ratio of ultimate to first yield deflection, where Δ_u is the deflection at ultimate moment and Δ_y is the deflection when steel yields. In general, high ductility ratios indicate that a structural member is capable of undergoing large deflections prior to failure. One of the factors contributing to the good ductility behaviour of the GPC beams was the good bonding of GPC with steel reinforcement. Ashour (2000) mentions that members with a displacement ductility in the range of 2 to 5 has adequate ductility and can be considered for structural members subjected to large displacements, such as sudden forces caused by earthquake.

Table 5.8 Displacement Ductility of beams obtained from experiment

Beam no.	Yield stage		Ultimate stage		Displacement ductility ratio Δ_u/Δ_y
	Moment(KNm)	Deflection Δ_y (mm)	Moment(KNm)	Deflection Δ_u (mm)	
PPC-B1	5.92	1.69	8.86	2.91	1.72
GPC-B1	4.93	1.61	7.88	2.77	1.72
PPC-B2	6.75	3.51	9.75	7.1	2.02
GPC-B2	6	4.55	8.25	7.28	1.6
PPC-B3	9.79	2.22	13.52	4.69	2.11
GPC-B3	7.88	2.69	12.52	5.98	2.22

5.4 COLUMNS

5.4.1 General Observations

Structural frames are constructed from a series of interconnected slabs, beams, walls and columns. The primary purpose of the columns is to transfer the loads in a vertical direction to the foundation. In braced frames, i.e. those in which the lateral loading is transferred by structural elements such as shear walls, cores or bracing, the columns are subjected to axial loading in addition to moments induced by dead and live loads. Compression members can be classified as either short or long (slender) members, depending on their behaviour. If the second-order stresses due to transverse deformations affect the ultimate strength of a member, then the member is classified as a long member. If the transverse deformations are negligibly small, the ultimate strength is not affected by secondary moments, and the member is classified as a short member. In short column, slenderness effects and the associated the secondary moments are insignificant. Therefore, the column capacity is governed by the sectional capacity. On the other hand, columns with very high slenderness ratio are in danger of buckling (accompanied with large deflection) under relatively low compressive loads and there by failing suddenly. Short column fails in concrete crushed and bursting. Outward pressures break horizontal ties and bend vertical reinforcements. The failure mode of the short column is shown in Figure 5.10.

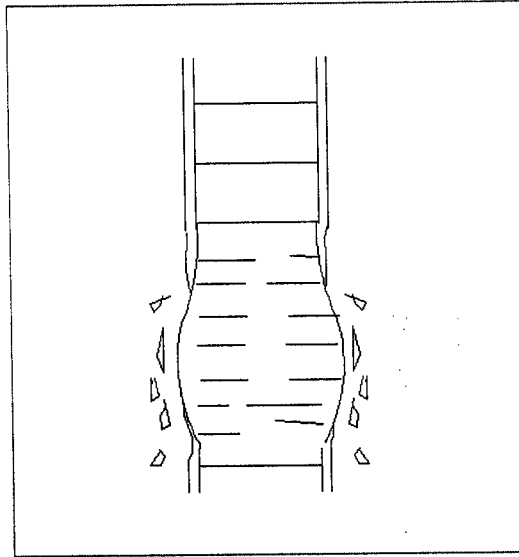


Figure 5.10 Failure Mode of Short Column

5.4.2 Load Carrying Capacity

Under axial loading, short columns are failing primarily by crushing or direct stresses and whole ultimate load carrying capacity is consequently independent of member length. When the load is applied to the centroid of the cross section of the loaded element, uniform compressive stresses of magnitude $f_a = P_{max}/A$ are developed. Failure occurs when the actual direct stress exceeds the crushing strength of material (i.e. $f_a > f_y$), where A is the cross sectional area of the column and f_y is the yield or crushing stress of the material. The maximum loads taken by the test specimens are compared with maximum load obtained theoretical calculation are tabulated in Table 5.9. Test data for column given in Appendix A.

Table 5.9 Ultimate load of test column specimen

Column no.	(1) $P_{\max(\text{exp})}$ (KN)	(2) $P_{\max(\text{theo})}$ (KN)	(1)/(2)
PPC-C1	148	147	1.01
PPC-C2	158	155	1.02
GPC-C1	126	147	0.86
GPC-C2	145	159	0.91

5.4.3 Axial Stress-Strain Curve for PPC-C1 and GPC-C1

Figure 5.11 represents typical stress-strain curve for uniaxially loaded short column. The curve to the right represents the axial stress (f_c) versus axial strain (ϵ_c) response, whereas the curve to the left shows the axial stress versus lateral strain (ϵ_l) relationship. As axial loading is increased, axial shortening of the column increases up to about 80 percent of the ultimate load. For axial strain values greater than $\epsilon_{c\text{limi}}$, the existing level of cracking of the concrete is seen as inducing nonlinear effects in the behavior of the material. Figure 5.12 shows the axial stress-strain curve for PPC-C1 and GPC-C1 column specimen. The axial shortening of column is measured by using the LVDT.

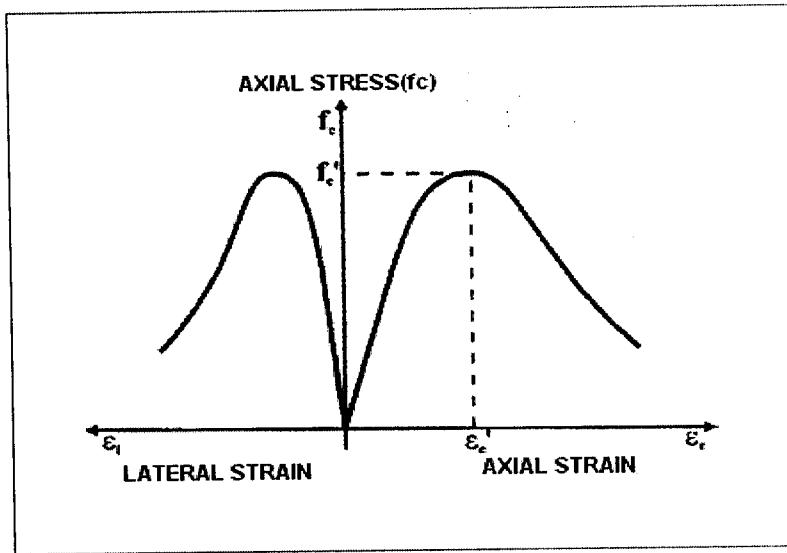


Figure 5.11 Typical stress-strain curves for uniaxially loaded short column

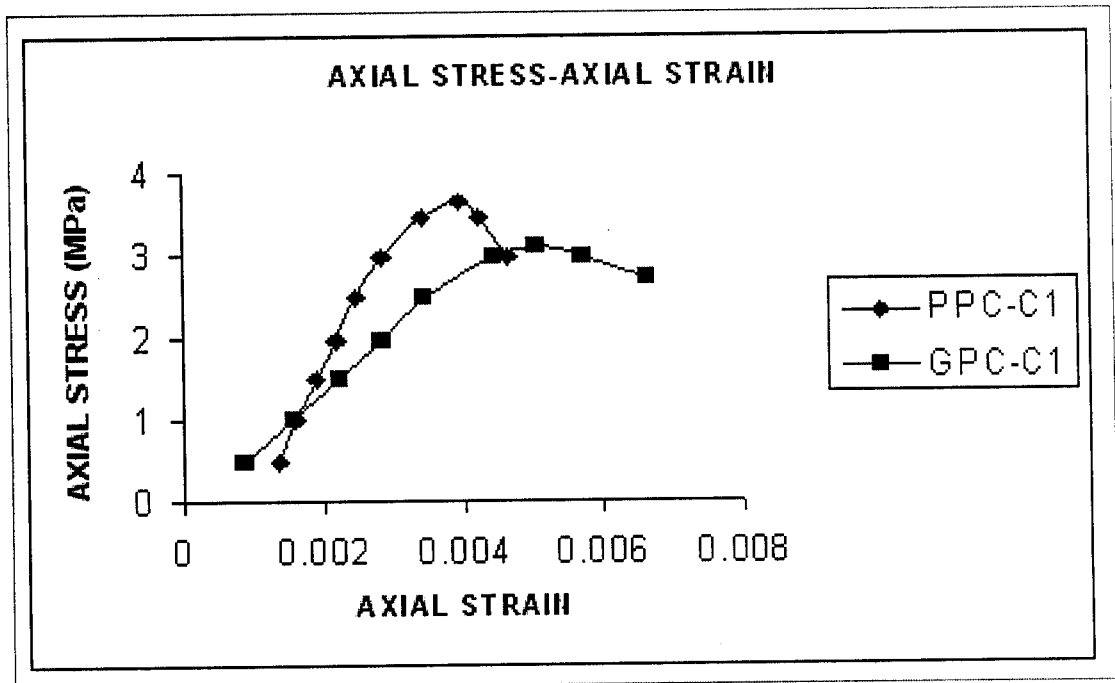


Figure 5.12 Axial stress-strain curves for PPC-C1 and GPC-C1 Column specimen

5.4.4 Axial Stress-Strain Curve for PPC-C2 and GPC-C2

Figure 5.13 shows the axial stress-strain curve for PPC-C2 and GPC-C2 column specimen. The axial shortening is measured by using the LVDT. Axial stress-strain plot of each column shown in Appendix C.

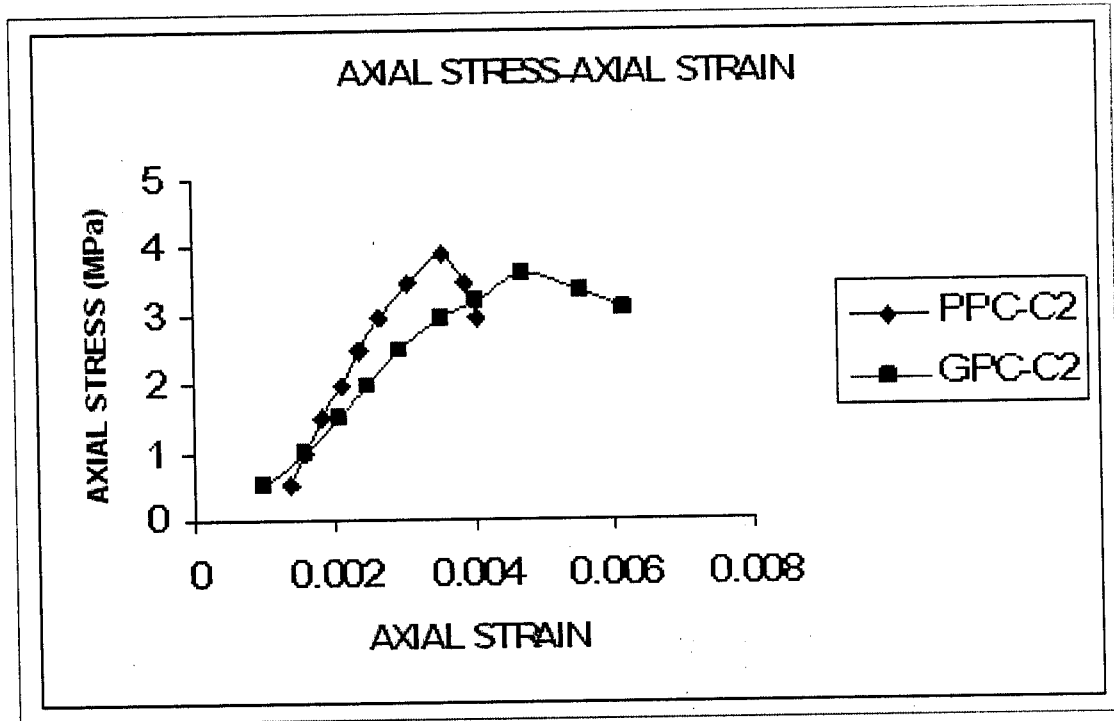


Figure 5.13 Axial stress-strain curves for PPC-C2 and GPC-C2
Column specimen

5.4.5 Crack Pattern and Failure Mode

The concrete cover started to fall away due to lateral dilation under the loading. However, even after the concrete cover had spalled, the confined core continued to carry an increasing load. The final sudden failure of this column was due to the yielding of steel reinforcement. Typical failure modes of test column are presented in Figure 5.14 and Figure 5.15

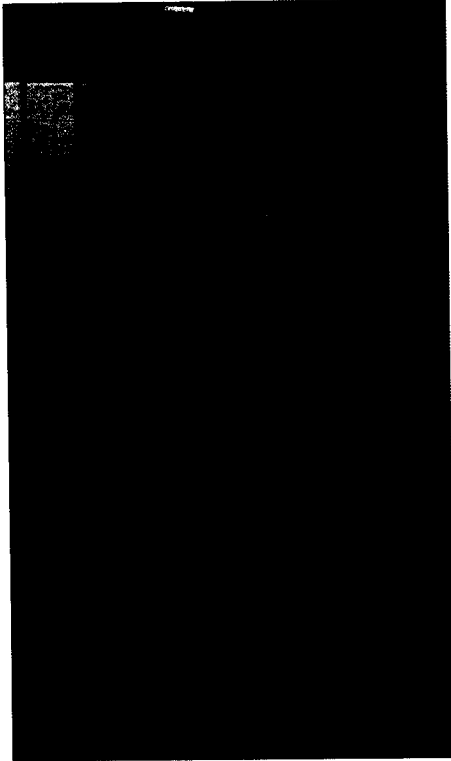


Figure 5.14 Failure mode of GPC-C1

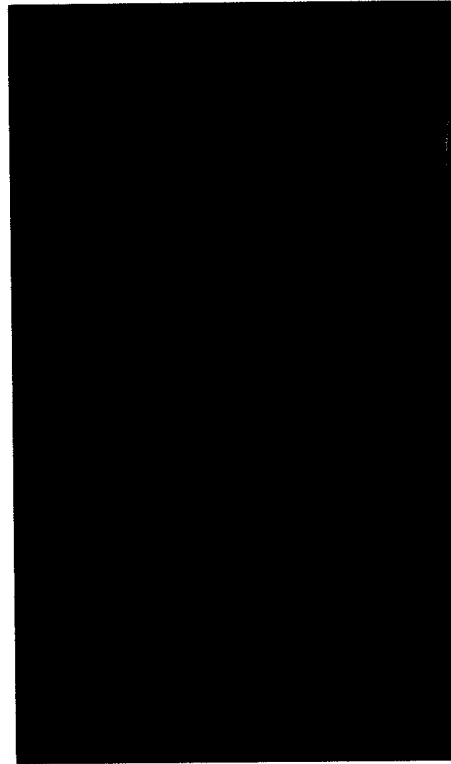


Figure 5.15 Failure mode of PPC-C1

CONCLUSIONS



CHAPTER 6

CONCLUSIONS

6.1 GENERAL CONCLUSION

The following conclusions were made within the limitation of experimental investigation.

1. Steam cured fly ash based geopolymer concrete has less strength than oven cured geopolymer concrete.
2. There is no substantial gain in the compressive strength of steam-cured fly ash based geopolymer concrete with age.
3. The GPC made from locally available sodium silicate is found to be cheaper than the conventional concrete.
4. The higher the ratio of silicate-to-sodium hydroxide liquid ratio by mass, higher is the compressive strength of Geopolymer Concrete
5. The workability for geopolymer concrete (GPC) is low, when compared with the conventional concrete.
6. As there are no codes that specify standards for geopolymer concrete, the mixes should be designed, experimented and then used, as the quality of fly ash used plays very important role in it.

6.2 SPECIFIC CONCLUSION

6.2.1 Reinforced Geopolymer Concrete Beams

From the experimental and analytical studies the following conclusions are drawn:

1. The crack patterns observed for reinforced geopolymer concrete beams were similar to those for reinforced Portland cement concrete beams. All beams failed in flexure in a ductile manner accompanied by crushing of the concrete in the compression zone.
2. The cracking moments of reinforced geopolymer concrete beams were calculated using the design provisions in ACI 318. The mean value of test/calculated cracking moments is 1.39.

3. All beams showed typical structural behaviour in flexure. Since the beams were under reinforced, yielding of the tensile reinforcement occurred before crushing of the compression concrete in the pure bending zone.
4. The ductility of reinforced geopolymer concrete beams is indicated by the ratio of mid-span deflection at ultimate moment-to-mid-span deflection at yield moment. All beams showed good ductility behaviour. And beams exhibited considerable amount of deflection, which provided ample warning to the imminence of failure. These test trends are comparable to the behaviour of reinforced Portland cement concrete beams.
5. The flexural capacity of test beams were calculated using the flexural design provisions contained in IS 456:2000. Good correlation is found between the test and calculated ultimate bending moments.
6. The study demonstrated that the design provisions contained in the IS 456: 2000 are applicable to reinforced geopolymer concrete beams.

6.2.2 Reinforced Geopolymer Concrete Columns

From the experimental and analytical studies the following conclusions are drawn:

1. The crack patterns and failure modes observed for geopolymer concrete short columns were similar to those reported in the literature for reinforced Portland cement concrete columns. Flexural cracks initiated at column mid-height, followed by cracks along the length of the column. The mode of failure was flexural, as indicated by opening of the cracks and the crushing of the concrete in the compression zone.
2. As expected, the capacity of test columns was influenced by the lateral tie spacing. The failure load of test columns increased as the lateral tie spacing is increased.
3. The load capacity of test columns was calculated using design provision in IS 456-200 for reinforced Portland cement concrete columns. Good correlation between test and calculated failure loads is found. The mean value of test failure load/calculated failure load is 0.95.
4. The study demonstrated that the design provisions contained in the IS 456-2000 and the American Concrete Institute Building Code ACI318-02 are applicable to reinforced geopolymer concrete columns.

REFERENCES



REFERENCES

- [1] ACI 318-02 (2002) "Building Code Requirements for Structural Concrete." Reported by ACI Committee 318, American Concrete Institute, Farmington Hills, MI.
- [2] ACI 232.2R-03 (2003) "Use of Fly Ash in Concrete." Reported by ACI Committee 232, American Concrete Institute, Farmington Hills, MI.
- [3] ASTM C78-02 Standard test method for flexural strength of concrete
- [4] B. Vijaya Rangan (2008) Mix design and production of flyash based geopolymer concrete The Indian Concrete Journal May, p 7
- [5] D. M. J. Sumajouw, D. Hardjito, S. E. Wallah, B. V. Rangan (2007) Fly ash-based geopolymer concrete: study of slender reinforced columns J Mater Sci (2007) 42:3124–3130
- [6] D.S. Perera, O. Uchida, E.R. Vane, K.S. Finnie (2007) Influence of curing schedule on the integrity of geopolymers J Mater Sci (2007) 42:3099–3106
- [7] D. Hardjito, Wallah SE, Sumajouw DMJ, Rangan BV (2004) J ACI Mater, p 467
- [8] Hardjito, D. and Rangan, B.V. (2006). Development and properties of low calcium fly ash based geopolymer concrete. Research report GC-1, Faculty of Engineering, Curtin University of Technology, Perth, Australia.
- [9] IS: 383-1970. Specifications for coarse and fine aggregates from natural sources for concrete. Bureau of Indian Standards, NewDelhi.
- [10] IS: 1727-1967. Method of tests for pozzolanic materials. Bureau of Indian Standards, NewDelhi

- [11] IS: 516-1959. Methods of tests for strength of concrete. Bureau of Indian Standards, NewDelhi
- [12] IS 456:2000, Plain and reinforced concrete-code of practice, Bureau of Indian standards, NewDelhi
- [13] Malhotra VM (2002) ACI Concrete Int 24:22
- [14] N.P Rajamane, N. Lakshmanan, M.C. Nataraja (2009) Studies on geopolymer concretes having flyash based light weight aggregates, CE&CR February, p70
- [15] Rangan, B.V., Wallah, S.E. (2006). Low-calcium fly ash based geopolymer concrete: long term properties. Research report GC-2, Faculty of Engineering, Curtin University of Technology, Perth, Australia

APPENDIX



APPENDIX A

TEST DATA

A.1 BEAMS

Table A.1.1 Test data beam PPC-B1

Load(KN)	Mid-span deflection (mm)
6.59	.075
13.33	0.97
19.78	1.12
26.37	1.31
32.89	1.51
39.44	1.69
45.99	2.05
52.52	2.44
59.05	2.91
52.52	2.99
45.99	3.25

Table A.1.2 Test data beam PPC-B2

Load(KN)	Mid-span deflection (mm)
5	0.83
10	1.07
15	1.47
20	1.8
25	2.1
30	2.45
35	2.83
40	3.1
45	3.51
50	4.1
55	4.6
60	5.52
65	7.1
60	7.27
55	7.87

Table A.1.3 Test data beam PPC-B3

Load(KN)	Mid-span deflection (mm)
6.59	0.145
13.33	0.3
19.78	0.48
26.37	0.69
32.89	0.91
39.44	1.16
45.98	1.42
52.52	1.66
59.05	1.97
65.28	2.22
71.41	2.65
77.48	3.23
83.47	3.76
90.13	4.69
83.47	5.3
77.48	6.4
71.44	7.2

Table A.1.4 Test data beam GPC-B1

Load(KN)	Mid-span deflection (mm)
6.59	0.75
13.33	0.95
19.78	1.15
26.37	1.4
32.89	1.61
39.44	1.97
45.99	2.41
52.52	2.77
45.99	2.93
39.44	3.4

Table A.1.5 Test data beam GPC-B2

Load(KN)	Mid-span deflection (mm)
5	1.48
10	1.75
15	2.11
20	2.45
25	2.93
30	3.41
35	3.88
40	4.55
45	5.42
50	6.51
55	7.28
50	7.65
45	8.91

Table A.1.6 Test data beam GPC-B3

Load(KN)	Mid-span deflection (mm)
6.59	0.13
13.33	0.5
19.78	0.81
26.37	1.13
32.89	1.4
39.44	1.72
45.98	2.11
52.52	2.69
59.05	3.22
65.28	4.06
71.41	4.72
77.48	5.32
83.47	5.98
77.48	6.19

A.2 COLUMNS

Table A.2.1 Test data column PPC- C1

Axial stress(MPa)	Axial strain
0.494	0.0013
0.987	0.0016
1.481	0.0018
1.975	0.0022
2.469	0.0025
2.963	0.0028
3.457	0.0034
3.654	0.004
3.457	0.0042
2.962	0.0046

Table A.2.2 Test data column PPC-C2

Axial stress(MPa)	Axial strain
0.494	0.0014
0.988	0.0016
1.482	0.0018
1.975	0.0021
2.469	0.0024
2.963	0.0026
3.457	0.0031
3.901	0.0036
3.457	0.0039
2.962	0.0041

Table A.2.3 Test data column GPC-C1

Axial stress(MPa)	Axial strain
0.494	0.0009
0.988	0.0016
1.482	0.0022
1.975	0.0028
2.469	0.0035
2.962	0.0044
3.111	0.0050
2.962	0.0057
2.716	0.0066

Table A.2.4 Test data column GPC-C2

Axial stress(MPa)	Axial strain
0.494	0.0009
0.988	0.0017
1.482	0.0021
1.975	0.0025
2.469	0.0029
2.962	0.0036
3.209	0.0041
3.580	0.0047
3.333	0.0055
3.086	0.0062

APPENDIX B

LOAD-DEFLECTION GRAPHS

B.1 BEMS

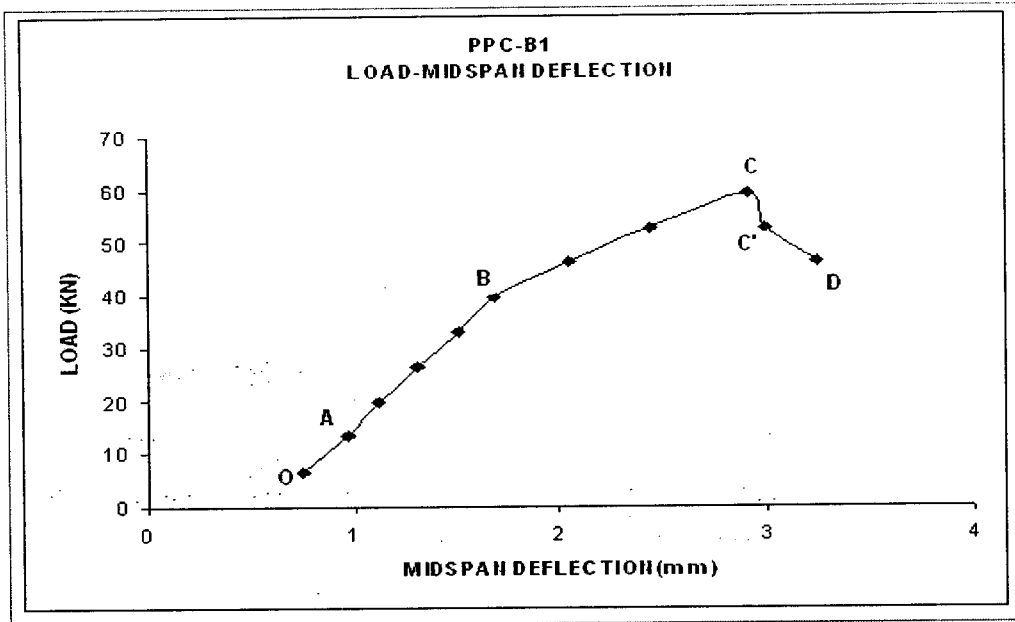


Figure B.1.1 Load versus deflection curve of PPC-B1

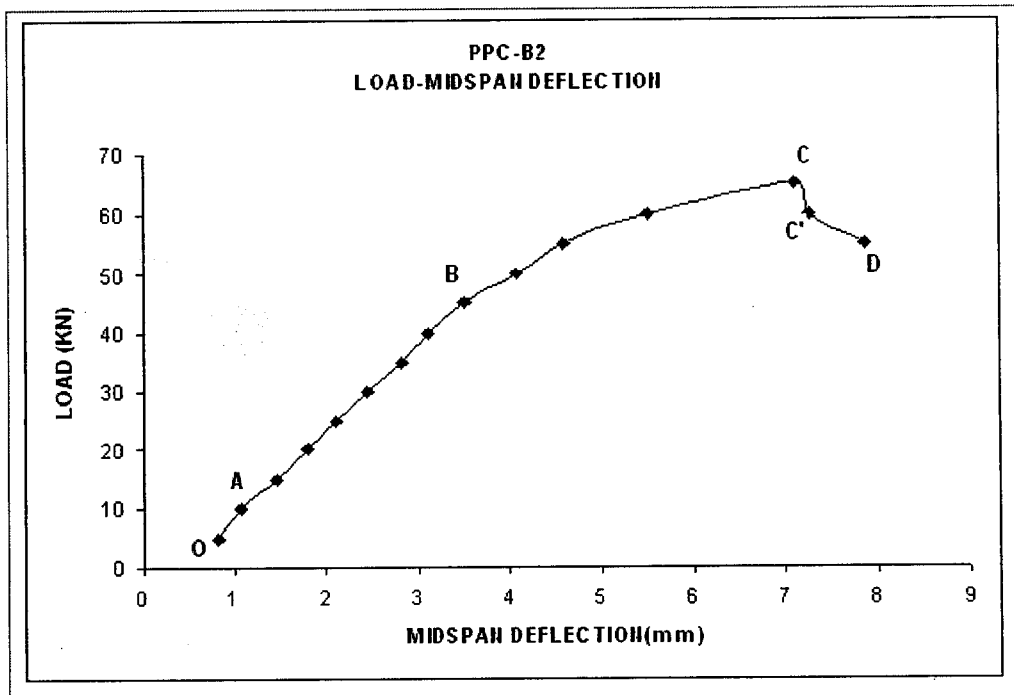
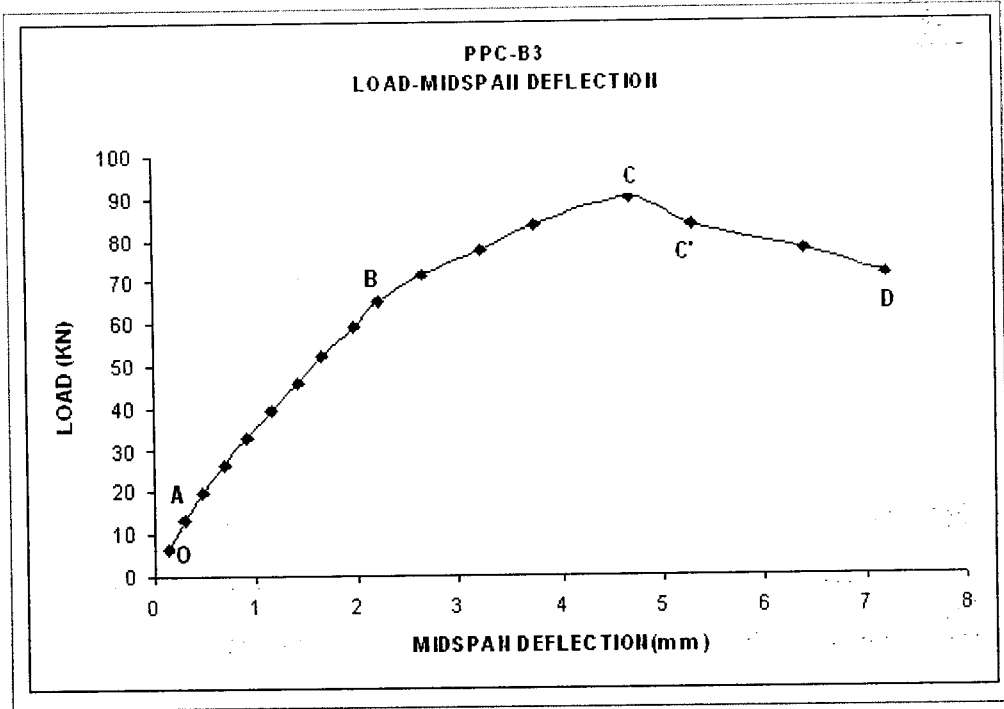
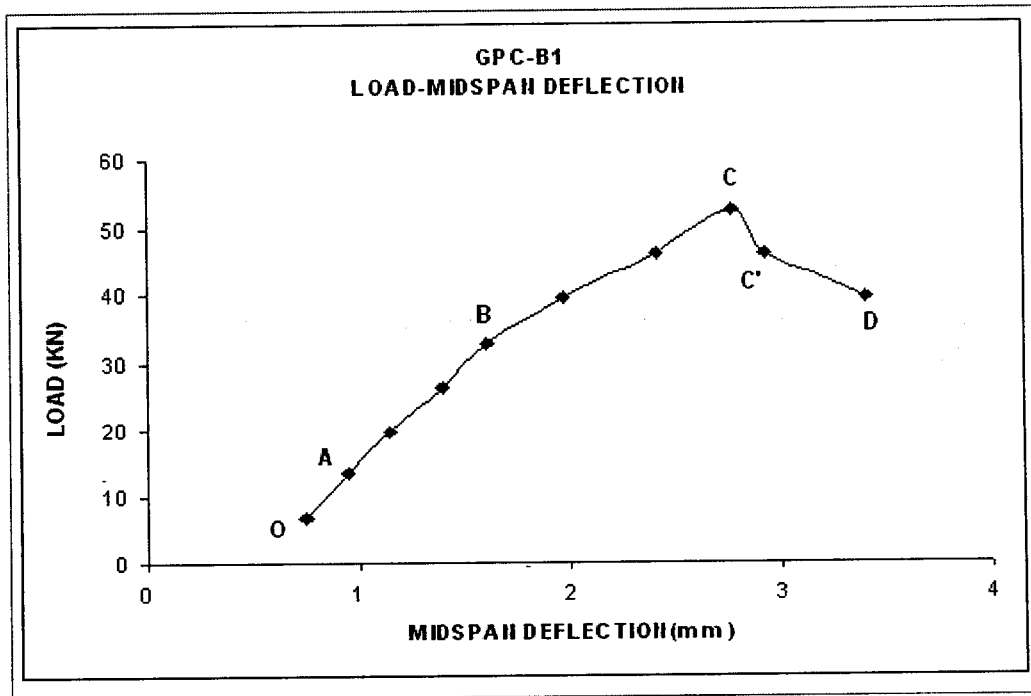


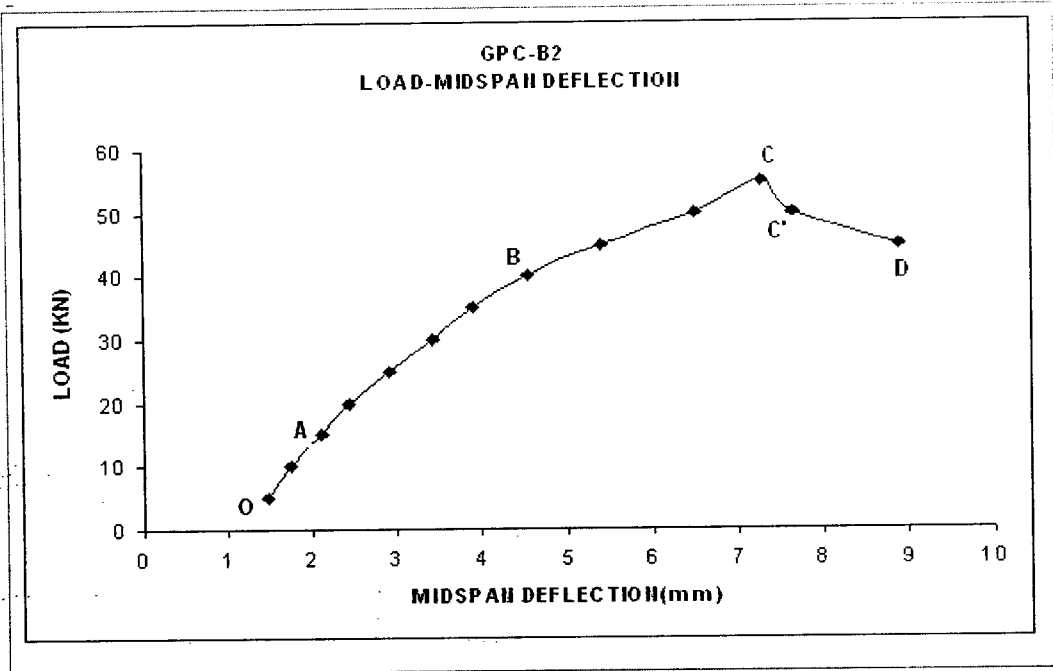
Figure B.1.2 Load versus deflection curve of PPC-B2



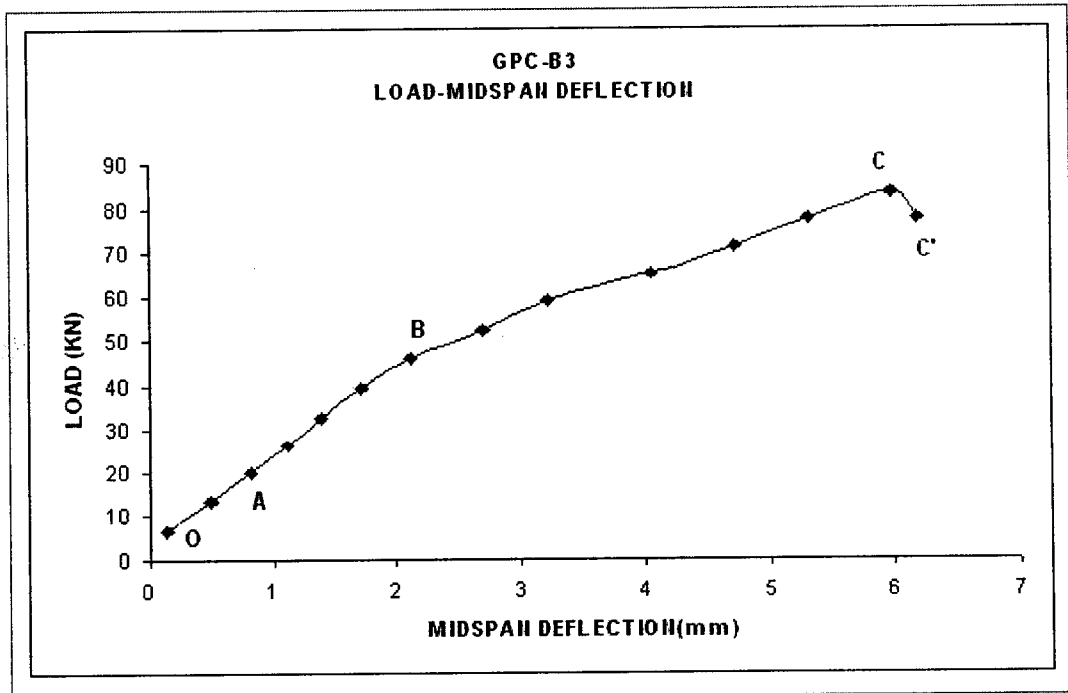
FigureB.1.3 Load versus deflection curve of PPC-B3



FigureB.1.4 Load versus deflection curve of GPC-B1



FigureB.1.4 Load versus deflection curve of GPC-B2

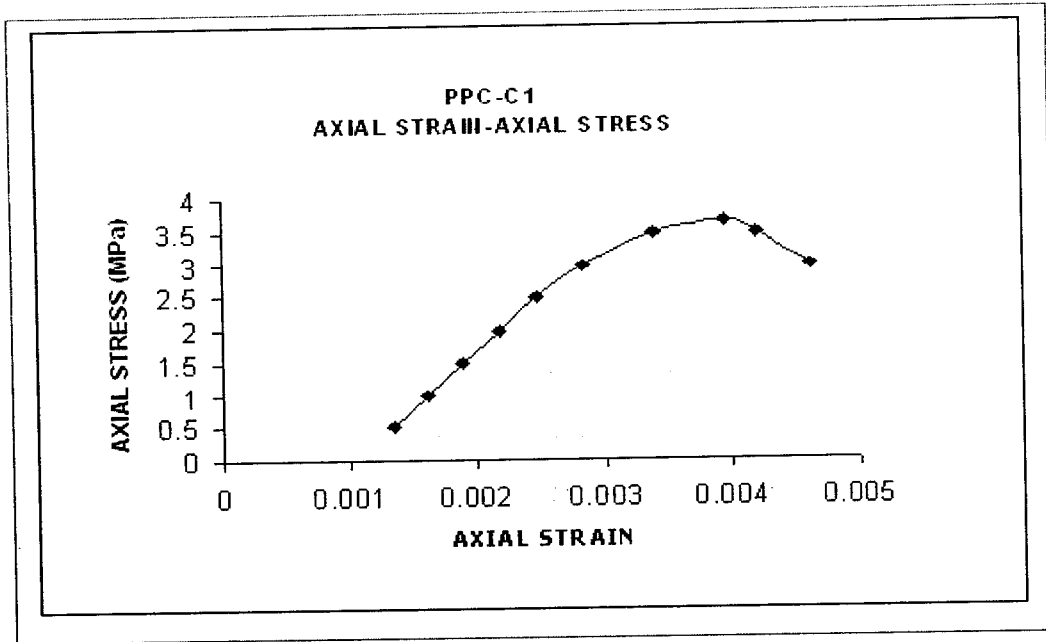


FigureB.1.6 Load versus deflection curve of GPC-B3

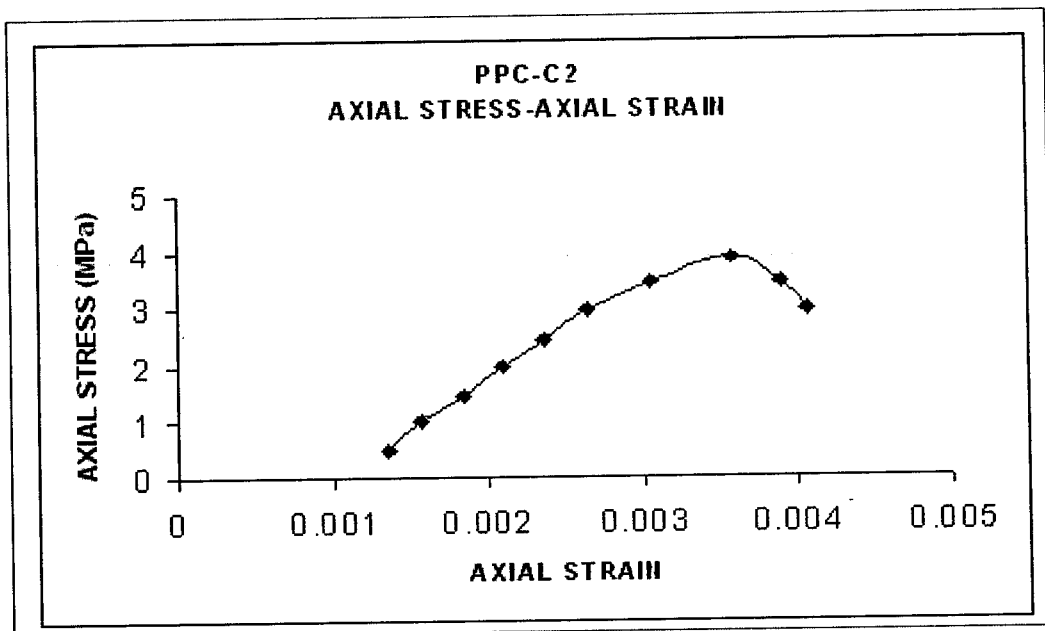
APPENDIX C

AXIAL STRESS-STRAIN GRAPHS

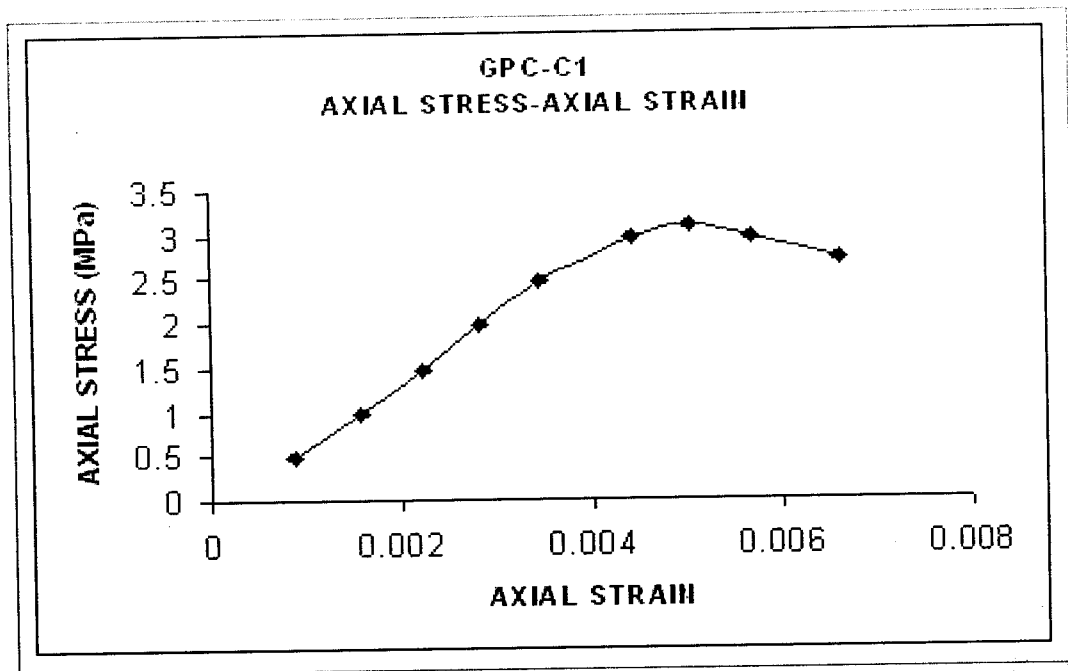
C.1 COLUMNS



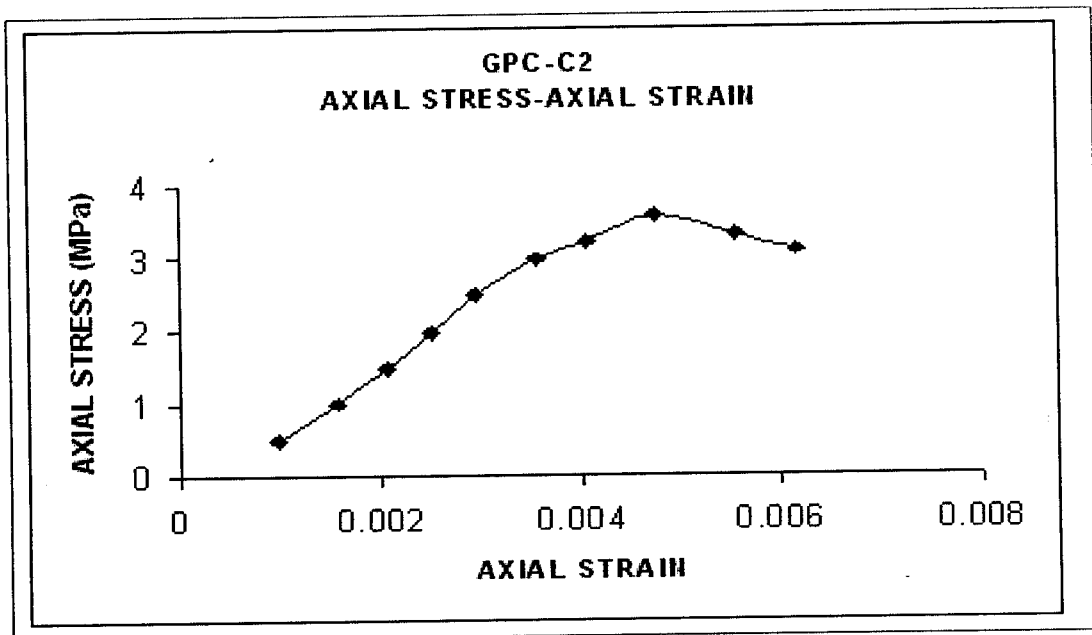
FigureC.1.1 Axial stress-axial strain curve PPC-C1



FigureC.1.2 Axial stress-axial strain curve PPC-C2



FigureC.1.3 Axial stress-axial strain curve GPC-C1



FigureC.1.2 Axial stress-axial strain curve GPC-C2

APPENDIX D

TEST RESULT OF SODIUM SILICATE SOLUTION

	SITRA SILICON INDIA TESTING & RESEARCH AGENCY Coimbatore Aerodrome Post, Coimbatore - 641 006 Dist. Coimbatore, Tamil Nadu Grens: SITRA Ph: (0422) 2574367-9, 6541488, 6544188 Fax: (0422) 2571625 Email: sitraindia@dataone.in Website: http://www.sitra.org.in Address all correspondence to the Director
XXIV/16721/08	04/08/2008
The Principal, Kumaraguru College of Technology P.B.No.2034 Coimbatore - 641 006 Tamilnadu	
Customer Reference	: dt.18.07.2008
Date of Receipt of Samples	: 18/07/2008
Test Report No.	: ChTR.No. : 1235
Sample Identification	: CH2217
TEST RESULTS	

Lab Code No. : CH2217	Sample Particulars : Liquid Sample

Density, g/cc	1.77
Purity of Sodium hydroxide as NaOH	15.01%
Purity of Sodium meta silicate as Na ₂ SiO ₃	59.38%
Solid content	69.33%
pH value	12.07

HOD/Lab Incharge Textile Chemistry	
Encl. : Bill	
N.B.: This report is strictly CONFIDENTIAL . Its use for publicity, arbitration or as evidence in legal disputes is forbidden. Reference of samples-sample given by the party. The above results are related to the samples tested. The report shall not be reproducible except in full without the written approval of the laboratory.	